

ARTICLE

Lipocalin-2 counteracts metabolic dysregulation in obesity and diabetes

Ioanna Mosialou^{1*}, Steven Shikhel^{1*}, Na Luo¹, Peristera Ioanna Petropoulou¹, Konstantinos Panitsas¹, Brygida Bisikirska¹, Nyanza J. Rothman¹, Roxane Tenta¹, Bertrand Cariou², Matthieu Wargny², Elisabeth Sornay-Rendu³, Thomas Nickolas⁴, Mishaella Rubin⁵, Cyrille B. Confavreux³, and Stavroula Kousteni¹

Regulation of food intake is a recently identified endocrine function of bone that is mediated by Lipocalin-2 (LCN2). Osteoblast-secreted LCN2 suppresses appetite and decreases fat mass while improving glucose metabolism. We now show that serum LCN2 levels correlate with insulin levels and β -cell function, indices of healthy glucose metabolism, in obese mice and obese, prediabetic women. However, LCN2 serum levels also correlate with body mass index and insulin resistance in the same individuals and are increased in obese mice. To dissect this apparent discrepancy, we modulated LCN2 levels in mice. Silencing *Lcn2* expression worsens metabolic dysfunction in genetic and diet-induced obese mice. Conversely, increasing circulating LCN2 levels improves metabolic parameters and promotes β -cell function in mouse models of β -cell failure acting as a growth factor necessary for β -cell adaptation to higher metabolic load. These results indicate that LCN2 up-regulation is a protective mechanism to counteract obesity-induced glucose intolerance by decreasing food intake and promoting adaptive β -cell proliferation.

Introduction

The discovery of the multiple endocrine functions of bone established a new paradigm whereby bone is a regulator of energy metabolism (Mera et al., 2018; Liu et al., 2018; Lee et al., 2007; Mera et al., 2016; Wei et al., 2014; Ferron et al., 2010; Yoshikawa et al., 2011). This subsequently raised the question of whether multiple bone-derived hormones may exist that contribute to glucose homeostatic functions such as glucose tolerance, insulin sensitivity, and energy expenditure or elicit unanticipated endocrine functions. In response to this question, a known hormone with a previously unclarified action on energy metabolism was found to mediate a new metabolic function of bone: regulation of food intake (Mosialou et al., 2017). Lipocalin-2 (LCN2) is a hormone that is expressed by osteoblasts in ≥ 10 -fold higher levels than in other tissues at basal states, and its osteoblast-specific inactivation in mice increases food intake, fat mass, and body weight (BW). In parallel, osteoblast-specific inactivation of *Lcn2* in mice leads to glucose intolerance, insulin resistance, and pancreatic β -cell dysfunction with a decrease in islet number and size, β -cell mass, and β -cell proliferation that results in reduced insulin secretion following glucose challenge. In

addition, chronic administration of exogenous LCN2 in lean and obese mice decreases food intake, fat mass, and BW gain and improves glucose metabolism, supporting a beneficial role for LCN2 in energy metabolism.

Other studies have proposed that LCN2 has a beneficial role in the regulation of various aspects of energy metabolism. Those include protection from diet-induced obesity, fatty liver disease, atherogenic dyslipidemia and insulin resistance, suppression of hepatic gluconeogenesis, and promotion of adaptive thermogenesis, activation of brown adipose tissue, and fatty acid oxidation (Guo et al., 2010, 2012, 2013; Paton et al., 2013; Zhang et al., 2014). In addition, normal-weight women whose LCN2 serum levels positively correlate with energy expenditure after a high-fat meal have improved fatty acid oxidation (Paton et al., 2013). Contrasting with this evidence, we note that elevated LCN2 serum levels have been associated with obesity and insulin resistance in mouse models and humans (Yan et al., 2007; Zhang et al., 2008; Wang et al., 2007; Kanaka-Gantenbein et al., 2008; Yoo et al., 2014; Rashad et al., 2017). Whether this increase in LCN2 levels is a cause or result of the metabolic dysregulation

¹Department of Physiology and Cellular Biophysics, Columbia University Medical Center, New York, NY; ²Université de Nantes, Centre Hospitalier Universitaire Nantes, Centre national de la recherche scientifique, Institut national de la santé et de la recherche médicale, l'Institut du thorax, Nantes, France; ³Institut national de la santé et de la recherche médicale Unités Mixtes de Recherche 1033, Université de Lyon, Hospices Civils de Lyon, Lyon, France; ⁴Department of Medicine Nephrology, Columbia University Medical Center, New York, NY; ⁵Department of Medicine Endocrinology, Columbia University Medical Center, New York, NY.

*I. Mosialou and S. Shikhel contributed equally to this paper; Correspondence to Stavroula Kousteni: sk2836@columbia.edu; Cyrille B. Confavreux: cyrille.confavreux@chu-lyon.fr.

© 2020 Mosialou et al. This article is distributed under the terms of an Attribution–Noncommercial–Share Alike–No Mirror Sites license for the first six months after the publication date (see <http://www.rupress.org/terms/>). After six months it is available under a Creative Commons License (Attribution–Noncommercial–Share Alike 4.0 International license, as described at <https://creativecommons.org/licenses/by-nc-sa/4.0/>).

and whether it has an impact on disease progression have not been examined. Moreover, although circulating LCN2 levels increase in obesity and insulin resistance associated with hyperglycemia in humans, its levels are decreased in patients with established type 2 diabetes (T2D) and are inversely correlated with BW and glycated hemoglobin in diabetic patients (De la Chesnaye et al., 2015; Mosialou et al., 2017; Wang et al., 2018). These observations suggest that more complex than anticipated mechanisms regulate LCN2 serum levels in lean or obese subjects, with or without diabetes. Therefore, they prompt an interrogation of what LCN2 serum levels may reflect in each situation and whether LCN2 may fulfill an additional function during the onset or progression of obesity and diabetes to its role during homeostasis.

In addressing this question, we traced changes in circulating LCN2 levels during the development of obesity and diabetes in mice and humans. We found that circulating LCN2 levels correlate with insulin levels and β -cell function, two indices of healthy glucose metabolism, in genetic and diet-induced mouse models of obesity and women with prediabetes. However, circulating LCN2 levels also correlate with body mass index (BMI) and insulin resistance in the same patients and are increased in obese mice. Silencing *Lcn2* expression in obese diabetic mice worsened metabolic dysfunction while chronically increasing its levels in healthy mice improves their metabolic profile. In addition, a beneficial effect of LCN2 on β -cell function was observed in two mouse models of β -cell failure, suggesting a distinct beneficial effect of LCN2 on adaptive β -cell proliferation during toxicity or onset of obesity.

Results

LCN2 correlates with β -cell function and insulin resistance in prediabetic women

To better understand the nature of the connection that exists between circulating LCN2 levels and obesity in the development of diabetes, we asked whether there was any correlation between fasting serum LCN2 levels and markers of glucose homeostasis in a 5-yr prospective study conducted in postmenopausal women with prediabetes ($n = 88$). Baseline subject characteristics are summarized in Table 1. In this population, there was no association between fasting plasma glucose and LCN2. In contrast, there was a strong positive correlation between serum LCN2 levels and BMI ($r = 0.30$; $P = 0.004$; Fig. 1 A), waist circumference ($r = 0.29$; $P = 0.006$; Fig. 1 B), serum insulin levels ($r = 0.39$; $P = 0.0004$; Fig. 1 C), and homeostatic model assessment of β -cell function (HOMA-B; $r = 0.39$; $P = 0.0003$; Fig. 1 D). Circulating LCN2 levels were also significantly correlated with indices of insulin resistance, i.e., homeostatic model assessment of insulin resistance (HOMA-IR; $r = 0.37$; $P = 0.0006$; Fig. 1 E). The correlations between serum LCN2 levels and BMI, waist circumference, and HOMA-IR became stronger when BMI was segregated into obese (BMI >30 kg/m 2 ; $n = 39$) and severely obese (BMI >35 kg/m 2 ; $n = 25$) groups (Table 2). There was also an inverse correlation between circulating LCN2 levels and serum adiponectin levels ($r = -0.29$; $P = 0.0096$; Fig. 1 F).

Table 1. Baseline characteristics of prediabetic women ($n = 88$)

Parameter	Mean \pm SEM
Age (yr)	56.2 \pm 10.8
BMI (kg/m 2)	32.2 \pm 8.3
Waist circumference (cm)	97.4 \pm 18.8
FBG (mmol/liter)	6.32 \pm 0.5
HbA1c (%)	6.0 \pm 0.4
Insulin (UI/ml)	15.6 \pm 9.3
LCN2 (ng/ml)	81.9 \pm 29.4
Adiponectin (μ g/ml)	4.85 \pm 2.88
HOMA-IR	4.43 \pm 2.86
HOMA-B	111.7 \pm 63.4

FBG, fasting blood glucose.

Furthermore, a logistic regression analysis showed that the increase of HOMA-IR is highly associated with the likelihood of belonging to the group of patients with the highest quartile of LCN2 levels (odds ratio [OR] = 2.81 per 1 SD increase [1.46–5.40]; $P = 0.002$). This remains even after adjustment on BMI (OR = 2.85 per 1 SD increase [1.32–6.16]; $P = 0.008$) or waist circumference (OR = 2.44 per 1 SD increase [1.16–5.14]; $P = 0.02$). During the 5-yr follow up, 33 patients (37.5%) developed T2D. Using a Cox model, we examined whether baseline serum LCN2 levels could predict such new-onset diabetes. Baseline fasting LCN2 levels were not associated with the risk of developing T2D (hazard ratio [HR] = 1.06 per 1 SD increase [0.72–1.55]; $P = 0.78$), whereas HOMA-IR was significantly associated with new-onset diabetes (HR = 1.48 [1.09–2.02]; $P = 0.01$).

We also analyzed circulating LCN2 levels in a different cohort of postmenopausal women with T2D ($n = 54$; Table 3) with an average duration of the disease (11 ± 1.3 yr) and similar age (59.4 ± 1.8 yr) and BMI (31.7 ± 0.9 kg/m 2) as the prediabetic group (age, 56.2 ± 0.8 yr; BMI, 32.2 ± 8.3 kg/m 2). We found that as disease progresses, the association of LCN2 with serum insulin levels and hemoglobin A1c (HbA1c) was reversed, showing a statistically significant negative association ($\beta_{\text{insulin}} = -0.002$, $P = 0.037$ and $\beta_{\text{HbA1c}} = -0.069$, $P = 0.032$, respectively; Table 4). This was not due to a lack of an increase in LCN2 levels in the diabetic state as LCN2 serum levels were similarly elevated in diabetic (87.28 ± 5.1 ng/ml), and prediabetic patients (81.9 ± 29.4 ng/ml; Fig. 1 G, Table 1, and Table 3). This increase was independent of BMI, as LCN2 serum levels were equally elevated among all three BMI groups as compared with lean healthy subjects (58.58 ± 7.61 ng/ml; Fig. 1 H). These results are reminiscent of the decrease in HbA1c with increasing LCN2 levels previously noted in men with T2D of similar age (Table S1; Mosialou et al., 2017). Linear regression analysis did not show any significant associations between circulating LCN2 levels and the rest of the metabolic parameters in this cohort of male T2D patients. This could be due to the small size of the sample ($n = 24$), the absence of non-T2D subjects in this group, or a possible gender-specific response for LCN2. However,

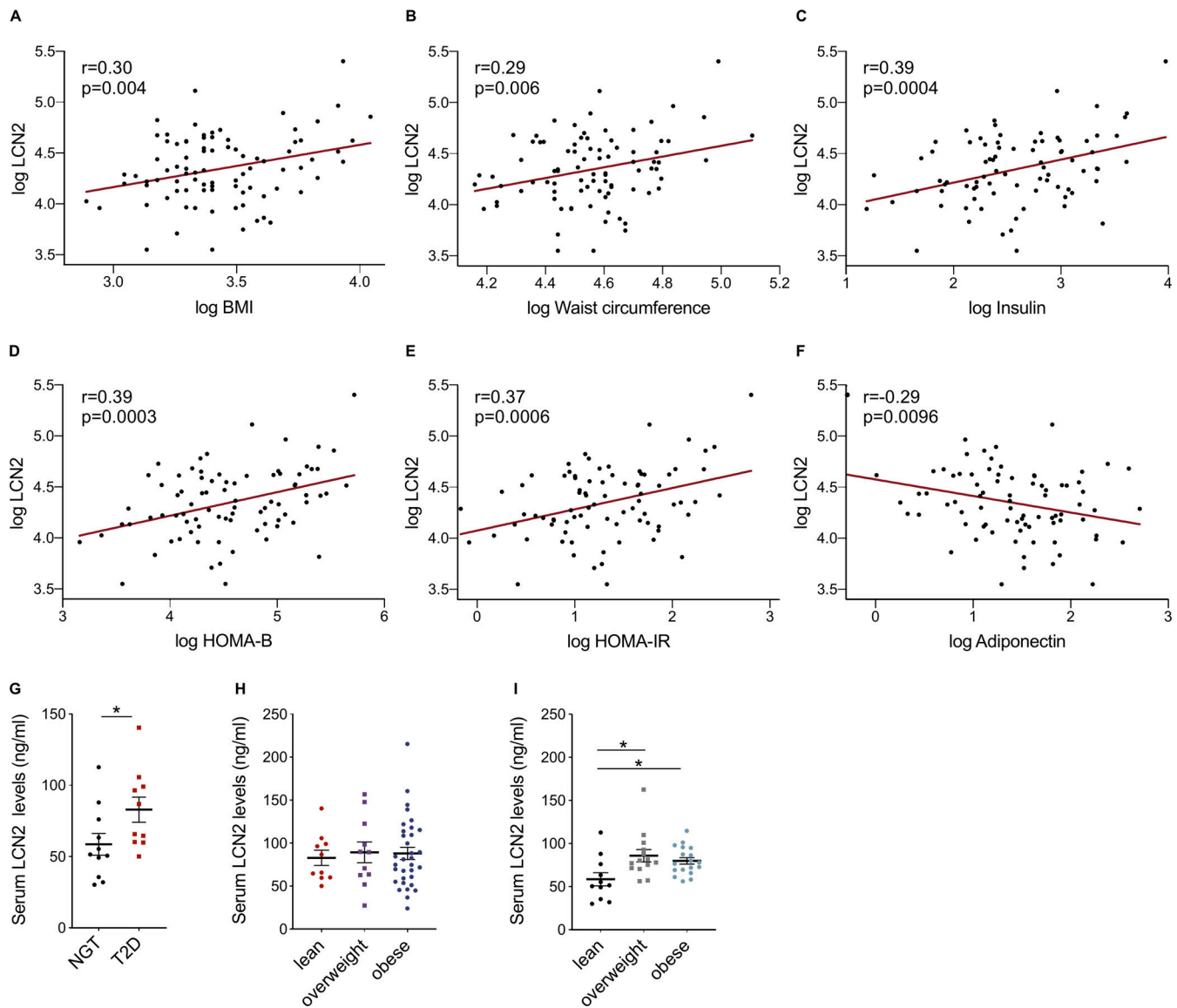


Figure 1. Circulating LCN2 levels correlate with obesity, insulin resistance, and β -cell function in prediabetic women and are elevated in obese and type 2 diabetic women. (A–F) Pearson correlations of morning fasting LCN2 serum levels with BMI (A), waist circumference (B), serum insulin levels (C), HOMA-B (D), HOMA-IR (E), and adiponectin levels (F) after log transformation of variables in prediabetic women ($n = 88$). **(G–I)** Serum LCN2 levels in postmenopausal women of varying BMI and diabetes status: (G) lean women with normal glucose tolerance (NGT; $n = 11$) versus lean T2D ($n = 10$) women, (H) T2D women segregated by BMI (lean, $n = 10$; overweight, $n = 11$; and obese, $n = 33$), and (I) women with NGT segregated by BMI (lean, $n = 11$; overweight, $n = 14$; and obese, $n = 18$). In G–I, normality of the data distribution was determined by the Kolmogorov–Smirnov test, and data are presented as mean \pm SEM. *, $P < 0.05$, Mann–Whitney test (G) and one-way ANOVA (H and I).

a positive correlation between circulating LCN2 levels and improved β -cell function was found, as measured by HOMA-B ($r = 0.5443$, $P = 0.006$; Fig. S1). Taken together, these results suggest that while increased circulating LCN2 levels are indicative of a metabolic deregulation at the onset of insulin resistance in the prediabetic state, they become indicative of a better metabolic regulation in the presence of insulin resistance in T2D. This biphasic association between LCN2 and the progression of the disease explains why LCN2 cannot be used to predict diabetes onset. It also suggests that LCN2 is unlikely to be a causative factor in disease progression. On the contrary, and in light of our previous observations of a beneficial role for LCN2 in

obesity and glucose metabolism in mice, the increase in LCN2 levels with the onset of insulin resistance most probably reflects a compensatory protective response for LCN2, increasing as glucose metabolism deteriorates to subsequently improve β -cell function and decrease hyperglycemia.

Serum LCN2 levels are increased in mouse models of obesity

To better understand the role of LCN2, if any, on the pathophysiology of diabetes, we next used genetic and diet-induced mouse models of obesity and T2D. The observations presented above and gathered in diabetic and obese prediabetic subjects prompted us to first examine whether LCN2 serum levels are

Table 2. **Strengthening of the correlation coefficients between LCN2 and BMI, waist circumference, and HOMA-IR according to BMI cutoff**

	BMI	Waist circumference	HOMA-IR
Whole population (n = 88)	0.30**	0.29*	0.37**
BMI >30 kg/m ² (n = 39)	0.49**	0.47**	0.41*
BMI >35 kg/m ² (n = 25)	0.61**	0.52*	0.51*

All variables were log transformed. *, $P \leq 0.01$; **, $P < 0.005$.

elevated in leptin-deficient (*Lepr^{ob/ob}*), leptin receptor-deficient (*Lepr^{db/db}*), melanocortin 4 receptor-deficient (*Mcr4^{-/-}*), and high-fat diet (HFD)-fed mice. We found that circulating LCN2 levels were twofold higher in 8-wk-old obese, insulin-resistant *Lepr^{ob/ob}* female mice (Fig. 2 A), *Lepr^{db/db}* male mice (Fig. 2 B), and 12- to 16-wk-old obese insulin-resistant *Mcr4^{-/-}* mice (Fig. 2 C) as compared with WT littermate controls. The increase in circulating LCN2 levels was evident as early as 5 wk of age in *Lepr^{db/db}* mice (Fig. 2 E), whereas circulating LCN2 levels in *Mcr4^{-/-}* mice became higher at 3 mo of age (Fig. 2 C). Circulating LCN2 levels were also 25% higher in WT male mice fed an HFD for 16 wk compared with littermate controls on regular chow diet (CD; Fig. 2 D). In HFD-fed mice, LCN2 levels started increasing within 4 wk of the start of the diet and became significantly different from those seen in mice fed a normal chow after 12 wk (Fig. 2 F). We note that this difference in the kinetics of the increase in circulating LCN2 levels in genetic and diet-induced models of obesity coincides with the differential onset of insulin resistance in each mouse model (Fig. 2, G–L), as determined by fed blood glucose levels >200 mg/dl. These results echo our findings in prediabetic subjects showing an increase in LCN2 serum levels in response to the development of impaired glucose metabolism and therefore indicate that mouse models could be used to further investigate the correlation between circulating LCN2 levels and obesity.

The increase in circulating LCN2 levels, at least upon HFD, is mainly contributed by bone, as the increase in serum LCN2 levels in these mice was lost following deletion of *Lcn2* in osteoblasts (*Lcn2^{osb}^{-/-}* mice; Fig. 3 A). *Lcn2* expression levels remained mainly unaltered in bone and all other tissues examined in all three mouse models of obesity (Fig. 3, B–D). A small

Table 4. **Linear regression analysis for indexes of glucose metabolism in postmenopausal NGT and T2D women**

Coefficient	Estimate	SE	t value	Pr(> t)
(Intercept)	3.757338***	0.377272	9.959	3.47e-16
Age (yr)	0.008894*	0.003903	2.279	0.0250
BMI (kg/m ²)	0.014321*	0.006784	2.111	0.0375
Diabetes	0.250008*	0.107071	2.335	0.0218
HbA1c (%)	-0.069224*	0.032201	-2.150	0.0343
Insulin	-0.002203*	0.001041	-2.115	0.0372
HOMA-IR	0.055218	0.034550	1.598	0.1135

*, $P < 0.05$; ***, $P < 0.001$. Residual SE, 0.3821 on 90 degrees of freedom. Multiple $R^2 = 0.1418$, adjusted $R^2 = 0.08456$. F-statistic, 2.478 on 6 and 90 degrees of freedom; $P = 0.02898$.

increase in *Lcn2* levels was observed in gonadal white adipose tissue and kidney of *Lepr^{ob/ob}* mice (Fig. 3 C) and liver and gonadal white adipose tissue of HFD-fed mice (Fig. 3 D). However, the lack of LCN2 increase in the serum of HFD-fed *Lcn2^{osb}^{-/-}* mice and the low *Lcn2* expression levels in kidney and liver as compared with marrow-free bone suggest that the contribution of these tissues to the increase in LCN2 levels in obesity is low (Fig. 3, C and D). Similarly, LCN2 protein levels were undetectable in the liver of WT or obese mice, while they were decreased in the bone and adipose tissue of *Lepr^{db/db}* and *Lepr^{ob/ob}* mice (Fig. 3 E). This was despite the lack of changes at the transcriptional level, suggesting that enhanced secretion from osteoblasts and white adipose tissue rather than transcriptional events may be involved in the elevation of serum LCN2 levels with obesity and diabetes. In support of this notion, combined treatment of osteoblasts with glucose and insulin induced the secretion of LCN2 (Fig. 3 F).

The positive correlation observed between circulating LCN2 levels and insulin resistance in obese and diabetic mice or the progression of diabetes suggests that the elevation in circulating LCN2 levels could be either a compensatory or driving response in the pathogenesis of insulin resistance. To examine this, we generated transgenic mice overexpressing *Lcn2* in osteoblasts (*Colla1-Lcn2^{Tg}*; Fig. S2 A). A 50% increase in circulating LCN2

Table 3. **Baseline characteristics of the T2D (n = 54) and non-T2D (n = 43) study population**

Parameter	Non-T2D (n = 43)			T2D (n = 54)		
	Lean (n = 11)	Overweight (n = 14)	Obese (n = 18)	Lean (n = 10)	Overweight (n = 11)	Obese (n = 33)
Age (yr)	61.63 ± 2.42	58.64 ± 1.80	61.38 ± 1.54	68.00 ± 2.77	65.36 ± 1.82	54.81 ± 2.45
BW (kg)	59.18 ± 1.90	69.48 ± 1.86	86.88 ± 2.26	52.90 ± 1.72	68.03 ± 1.93	92.41 ± 2.40
BMI (kg/m ²)	22.87 ± 0.64	27.07 ± 0.33	35.53 ± 0.79	21.55 ± 0.59	27.23 ± 0.38	36.30 ± 0.82
HbA1c (%)	5.68 ± 0.07	5.65 ± 0.08	5.90 ± 0.08	7.35 ± 0.26	8.31 ± 0.64	7.90 ± 0.35
FBG (mg/dl)	87.54 ± 2.12	88.85 ± 1.84	91.72 ± 2.46	118.90 ± 13.2	167.0 ± 23.79	160.81 ± 15.6
LCN2 (ng/ml)	58.58 ± 7.61	85.84 ± 7.09	79.88 ± 3.83	82.88 ± 8.84	89.21 ± 12.09	87.97 ± 7.04

Data are presented as means ± SEM. FBG, fasting blood glucose; HbA1c, glycated hemoglobin.

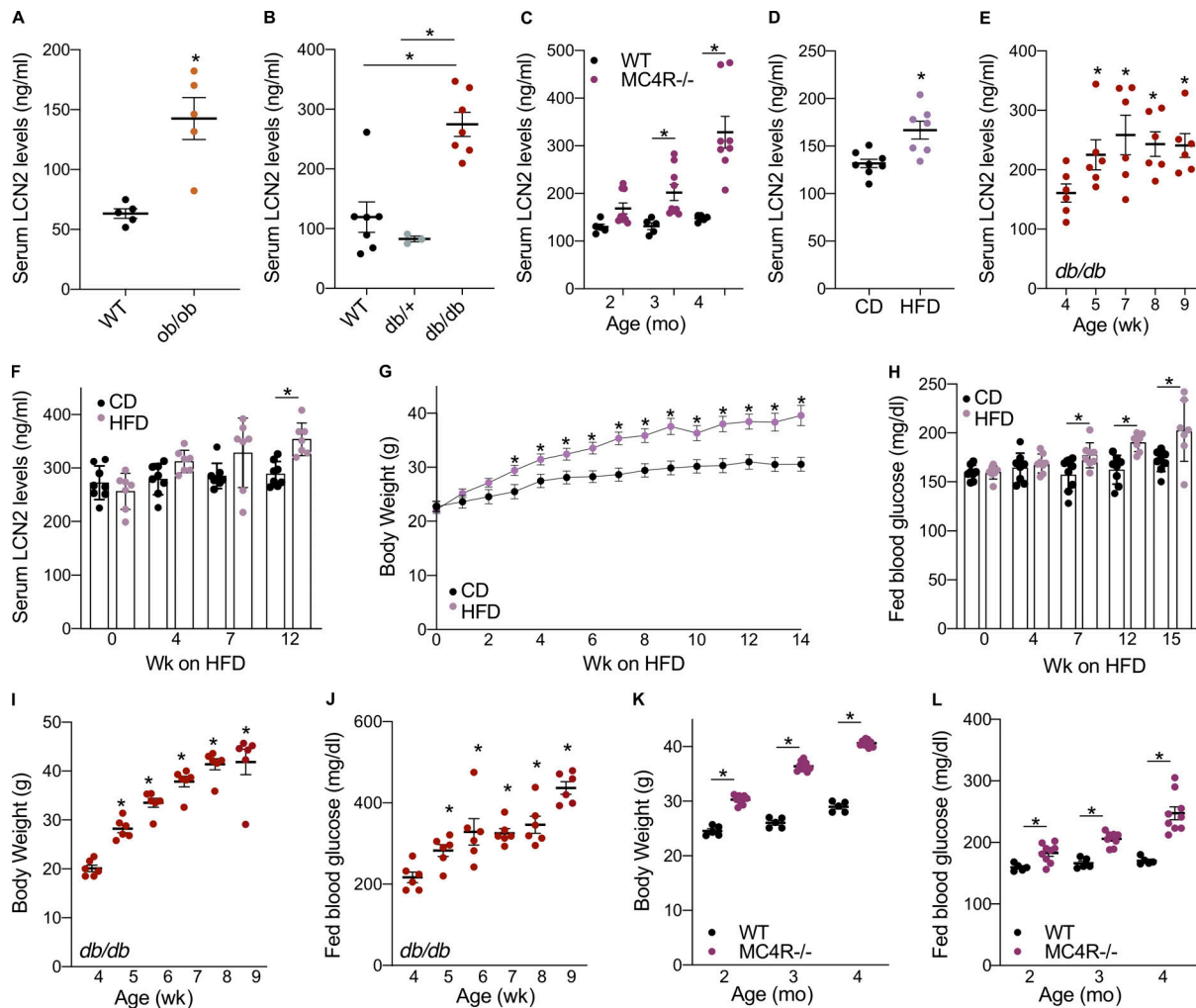


Figure 2. Circulating LCN2 levels are increased in mouse models of obesity and T2D. (A–F) Serum LCN2 levels in 8-wk-old female *Lepr^{db/db}* (n = 5) and WT littermates controls (n = 5; A); 8-wk-old male *Lepr^{db/+}* (n = 3), *Lepr^{db/db}* (n = 7), and WT littermates (n = 7; B); male *Mc4r^{-/-}* (n = 9) and WT littermates (n = 5) at 2–4 mo of age (C); male mice fed on HFD (n = 7) or regular CD (n = 8) for 16 wk starting at 8 wk of age (D); *Lepr^{db/db}* at 4–9 wk of age (n = 6; E); and HFD- (n = 7) or CD-fed (n = 8) mice after 4, 7, and 12 wk on diet (F). (G–L) BW and fed blood glucose levels in male mice fed on HFD (n = 7) or CD (n = 8) shown in D and F (G and H), male *Lepr^{db/db}* and littermate controls at 4–9 wk of age (n = 6) shown in E (I and J), and male *Mc4r^{-/-}* (n = 9) and WT littermate controls (n = 5) at 2, 3, and 4 mo of age shown in C (K and L). Data are representative of three independent experiments (A–L). Data are presented as mean ± SEM. *, P < 0.05 by Student's t test.

levels was observed in *Colla1-Lcn2^{Tg}* mice as compared with WT littermates (Figs. 4 A and S2 C). *Colla1-Lcn2^{Tg}* mice showed 12.5% decrease in food intake, decreased fat mass and BW, lower fed and fasting blood glucose levels, improved insulin sensitivity, and increased energy expenditure (Fig. 4, B–K). Both 3- and 6-mo-old *Colla1-Lcn2^{Tg}* mice showed increased expression of uncoupling protein 1 (*Ucp1*) and peroxisome proliferator-activated receptor gamma coactivator 1- α (*Pgc1a*) in brown adipose tissue compared with their WT littermates (Fig. 2, L and R), suggesting that the increase in energy expenditure is maintained at 6 mo of age. The fact that the improvement in metabolic parameters in the transgenic mice was observed as long as the mice were monitored (Fig. 4, M–Q) suggests that sustained elevated circulating LCN2 levels do not lead to obesity and insulin resistance but rather chronically suppress appetite and improve glucose metabolism.

To further clarify whether *Lcn2* overexpression is truly not deleterious to mice, we generated mice overexpressing *Lcn2* in

the liver (*apoE-Lcn2^{Tg}*; Fig. S2 B). These mice had eightfold increased serum LCN2 levels as compared with WT littermates (Fig. S2 D). Similar to *Colla1-Lcn2^{Tg}* mice, *apoE-Lcn2^{Tg}* mice showed a decrease in food intake, BW, and fat mass; lower fed and fasting blood glucose levels; improved glucose tolerance and insulin sensitivity; and increased energy expenditure (Fig. S2, E–O). No inflammation was observed based on white blood cell counts and expression of inflammatory cytokines in white adipose tissue (Fig. S2, P and Q). These results indicate that even higher sustained elevated circulating LCN2 levels are beneficial for energy metabolism.

LCN2 silencing worsens hyperphagia, glucose intolerance, and β -cell dysfunction of leptin receptor-deficient mice

Given the beneficial effects of LCN2 on food intake and β -cell function and the fact that elevated LCN2 levels in transgenic mice do not have any overt deleterious effect, we asked whether the increased circulating LCN2 levels are maintained in obese

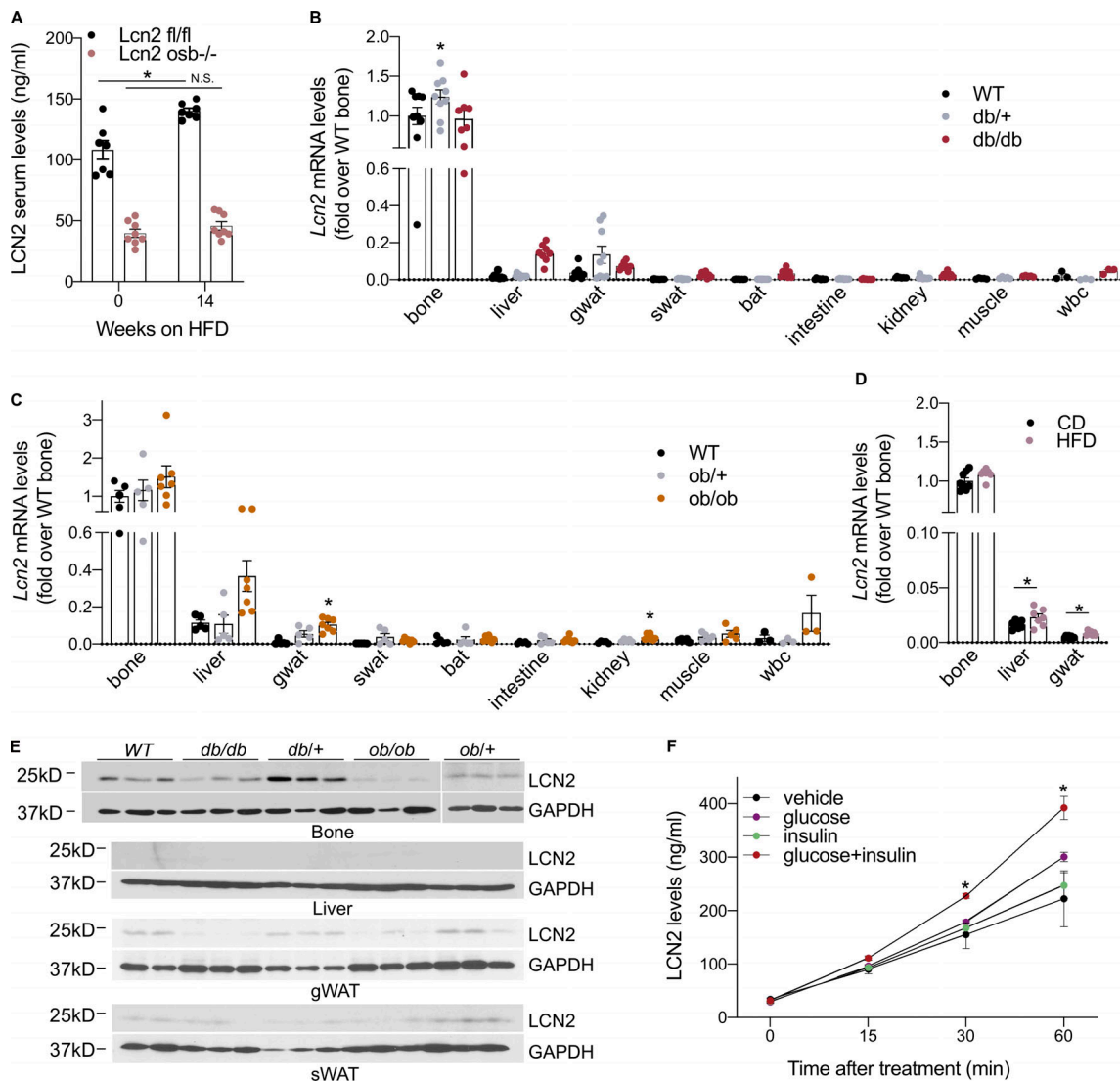


Figure 3. Enhanced LCN2 secretion from osteoblasts and adipocytes in mouse models of obesity and T2D. (A) Serum LCN2 levels in male *Lcn2^{osb}*^{-/-} (*n* = 8) and *Lcn2^{fl/fl}* (*n* = 7) littermate mice fed on HFD for 14 wk starting at 8 wk of age. (B–D) Real-time PCR analysis of *Lcn2* expression levels in the indicated tissues from 8-wk-old male WT mice (*n* = 8, apart from muscle [*n* = 5] and white blood cells [wbc; *n* = 3]), *Lepr^{db/+}* (*n* = 8, apart from muscle [*n* = 7] and white blood cells [*n* = 5]), and *Lepr^{db/db}* (*n* = 8, apart from muscle [*n* = 5] and white blood cells [*n* = 3]); 8-wk-old female WT mice (*n* = 5, apart from white blood cells [*n* = 3]), *Lepr^{ob/+}* (*n* = 5, apart from white blood cells [*n* = 3]), and *Lepr^{ob/ob}* (*n* = 7, apart from muscle [*n* = 5] and white blood cells [*n* = 3]); and mice fed on HFD (*n* = 7) or regular CD (*n* = 8) for 16 wk (D). (E) Western blot analysis of LCN2 levels in the indicated tissues from 8-wk-old WT, *Lepr^{db/db}*, *Lepr^{db/+}*, *Lepr^{ob/ob}*, and *Lepr^{ob/+}* mice (*n* = 3). In liver, gonadal white adipose tissue (gwat), and subcutaneous white adipose tissue (swat), *n* = 2 for WT mice. (F) LCN2 levels in cell culture supernatants of osteoblasts following treatment with glucose (4.5 g/liter), insulin (10 nM), or glucose and insulin for 15, 30, and 60 min. bat, brown adipose tissue; . Representative of three independent experiments (A–F). Data are presented as mean ± SEM. *, *P* < 0.05, Student's *t* test or two-way ANOVA (B and C).

mice as a protective mechanism against weight gain, β -cell failure, and glucose intolerance. For this purpose, *Lcn2* expression was silenced in *Lepr^{db/db}* mice by systemic delivery of *Lcn2* siRNA every 2 d for 30 d. This regimen decreased *Lcn2* expression levels in bone (30%), liver (50%), and adipose tissue (60%) and normalized its serum levels (Fig. 5, A and B).

We found that this 50% reduction in circulating LCN2 levels worsened the metabolic dysfunction in *Lepr^{db/db}* mice. Hyperphagia increased by 24%, leading to a 44% increase in gonadal fat pad weight, 50% increase in BW gain, and 6% increase in BW (Fig. 5, C–F). The size of these increases is in line with

observations following the loss of MC4R in *Lepr^{ob/ob}* mice (Trevaskis and Butler, 2005). Importantly, other hypoglycemic and insulinotropic agents induce changes similar to LCN2 (brain-derived neurotrophic factor) or even no changes at all (such as exendin-4, the long-acting glucagon-like peptide-1 (GLP-1) derivative NN2211, the precursor of bilirubin biliverdin, the GLP-1 receptor agonist ZP10A, or overexpression of the antioxidant glutathione peroxidase) in BW when administered to *Lepr^{db/db}* mice (Ono et al., 1997; Nakagawa et al., 2000; Greig et al., 1999; Ikeda et al., 2011; Rolin et al., 2002; Thorkildsen et al., 2003; Harmon et al., 2009). Fed and fasting blood glucose levels

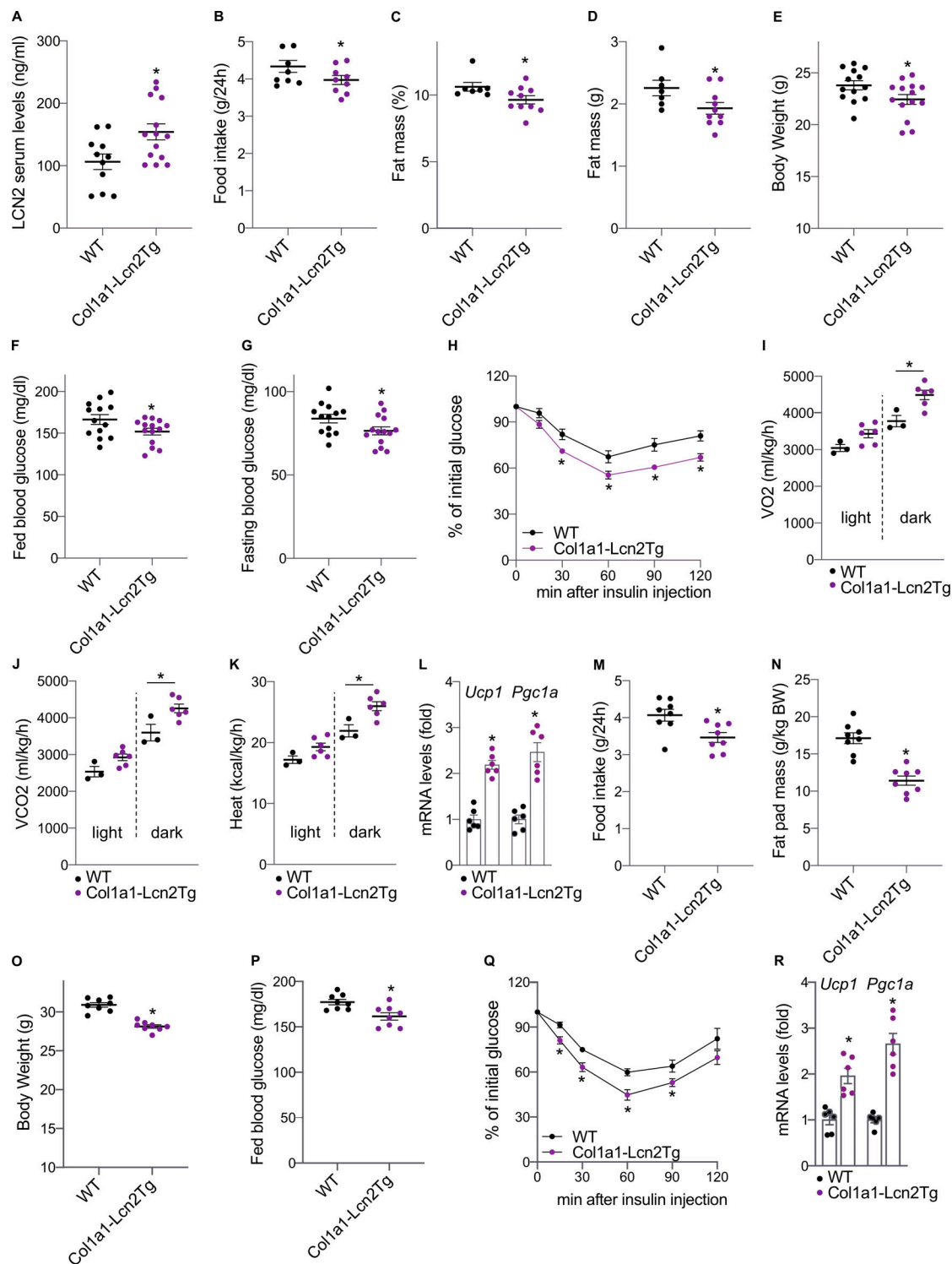
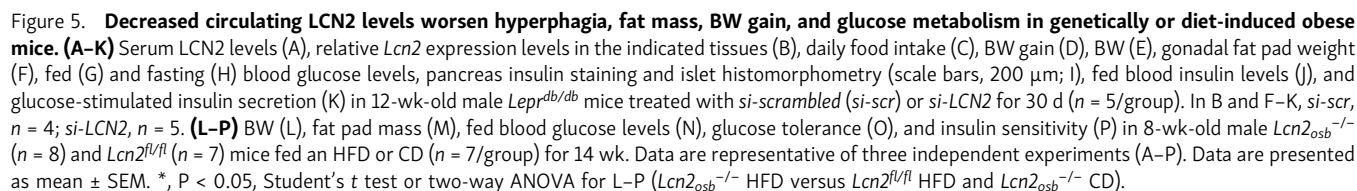


Figure 4. **Increased circulating LCN2 levels in mice overexpressing *Lcn2* in osteoblasts decreases food intake and fat mass and improves glucose metabolism.** (A–L) Serum LCN2 levels (A), daily food intake (B), fat body mass (percentage of total body mass; C), fat body mass (grams; D), BW (E), fed (F) and fasting (G) blood glucose levels, insulin sensitivity (H), O_2 consumption (I), CO_2 production (J), heat production (K), and relative expression levels of *Ucp1* and *Pgc1a* in brown adipose tissue of 10-wk-old *Col1a1-Lcn2^{Tg}* and WT littermate male mice (L). (M–R) Daily food intake (M), fat pad mass (N), BW (O), fed blood glucose levels (P), insulin sensitivity (Q), and relative expression levels of *Ucp1* and *Pgc1a* in brown adipose tissue of 6-mo-old *Col1a1-Lcn2^{Tg}* and WT littermate male mice (R). In A, WT, $n = 11$; *Col1a1-Lcn2^{Tg}*, $n = 14$. In B, $n = 9$ /group. In C and D, WT, $n = 7$; *Col1a1-Lcn2^{Tg}*, $n = 10$. In E–G, WT, $n = 13$; *Col1a1-Lcn2^{Tg}*, $n = 14$. In H, Q, L, and R, $n = 6$ /group. In I–K, WT, $n = 3$; *Col1a1-Lcn2^{Tg}*, $n = 6$. In M–P, $n = 8$ /group. Data are representative of three independent experiments (A–R). Data are presented as mean \pm SEM. *, $P < 0.05$, Student's t test.



Similarly, placing *Lcn2^{osb}^{-/-}* mice, which have 64% less circulating LCN2 levels, on HFD further worsened BW, fat pad mass, blood glucose levels, glucose intolerance, and insulin

resistance compared with WT littermate controls or lean *Lcn2^{osb}^{-/-}* mice (Fig. 5, L–P). Circulating LCN2 levels increased by 30% with HFD in WT mice but remained the same in *Lcn2^{osb}^{-/-}* mice (Fig. 3 A). These results indicate that the increase in LCN2 levels with obesity is mainly contributed by osteoblasts and, together with our previous data on *Lep^{db/db}* mice, substantiate the protective role of LCN2 during obesity.

LCN2 promotes adaptive β -cell proliferation and function in mouse models of diabetes and obesity

The positive association of serum LCN2 levels with insulin levels and β -cell function in obese, prediabetic, or diabetic patients and mouse models of obesity indicated that LCN2, in addition to limiting appetite, may also improve glucose handling in obesity by improving β -cell mass and function. To delineate whether LCN2 independently regulates obesity and β -cell phenotypes, we pair-fed *Lcn2^{osb}^{-/-}* mice to their WT littermates. We found that while pair-feeding normalized insulin sensitivity, BW, and fat mass and restored the suppression of lipolytic gene expression and the increase in the adipogenic gene expression program in *Lcn2^{osb}^{-/-}* mice, it did not rescue the impaired glucose-stimulated insulin secretion and serum insulin levels in *Lcn2^{osb}^{-/-}* mice, and as a result, their glucose intolerance persisted (Mosialou et al., 2017; Fig. S3, A–D). Moreover, LCN2 was able to directly act on mouse pancreatic islets and MIN6 pancreatic β -cells to increase insulin secretion (Mosialou et al., 2017) and promote β -cell proliferation (Fig. S3, E–I). Combined, these data suggest that there are two mechanisms involved in the protective role of LCN2 against diabetes, one limiting hyperphagia and thus reducing adiposity and BW and the other directly protecting β -cells and promoting β -cell proliferation.

To directly test this hypothesis, we first examined whether LCN2 acts as a growth factor for pancreatic β -cells in situations of extreme hyperglycemia. Mice were injected with a single high dose of streptozotocin (STZ) to induce β -cell death, and LCN2 was administered at day 8 after STZ injection, a time point at which blood glucose levels were >400 ng/ml (Fig. 6 A). This dose doubled LCN2 serum levels (Fig. S4 A) and has been shown to improve glucose metabolism and insulin sensitivity in healthy WT mice (Mosialou et al., 2017). In spite of the massive destruction of β -cells, LCN2 prevented STZ-induced lethality (defined as 20% BW loss, at which time point mice were moribund and euthanized; Fig. 6 B). Indeed, all mice treated with LCN2 survived whereas only 20% of vehicle-treated mice were alive two months after STZ treatment. In addition, LCN2 lowered fed and fasting blood glucose levels by day 16 following LCN2 treatment and increased islet number, β -cell area, β -cell mass, and serum insulin levels (Fig. 6, C–H; and Fig. S4 B). Similar to the single high dose of STZ, treatment with LCN2 of mice rendered diabetic with multiple low doses of STZ increased islet number, β -cell area, and β -cell mass as compared with STZ/vehicle-treated mice due to an increase in β -cell proliferation, leading to enhanced insulin secretion and serum insulin levels and improved blood glucose levels (Fig. 6, I–P). Interestingly, LCN2 serum levels were twice as high following multiple low doses of STZ as compared with a single high dose of STZ (Fig. S4 C). Different mechanisms in the two models (an immune cell

response in the multiple low-dose STZ model as compared with oxidative β -cell damage and apoptosis in the single high-dose STZ model) may have differentially regulated LCN2 levels. It is, however, possible that the smaller increase in circulating LCN2 levels with a single high dose of STZ as compared with multiple low doses of STZ may have contributed to the more severe phenotype developed following a single high dose of STZ.

Next, we examined whether LCN2 is necessary for β -cell adaptation to higher metabolic load by placing mice on HFD for 7 d. This has previously been shown to induce β -cell proliferation before any changes in insulin resistance and can be used to identify early drivers of β -cell proliferation (Stamateris et al., 2013). *Lcn2^{-/-}* and WT control mice were placed on HFD for 7 d, and subsequently, pancreata were collected and processed for histological analysis. BW and blood glucose levels increased comparably in both WT and *Lcn2^{-/-}* mice (Fig. 6, Q and R). However, whereas serum insulin levels increased by almost twofold in the WT mice, *Lcn2^{-/-}* mice failed to increase insulin production to meet increased metabolic demands (Fig. 6 S). As a result, glucose tolerance was significantly impaired in *Lcn2^{-/-}* as compared with WT mice by day 7 on HFD (Fig. 6 T). Histological analysis of the pancreas indicated that in *Lcn2^{-/-}* mice β -cell proliferation was decreased by half (Fig. 6 U and Fig. S4 D), indicating a potential lack of ability for hyperplasia. These results suggest that LCN2 is required to mount the early protective response that drives the proliferation of replication-refractory β -cells in mice fed on HFD to suppress hyperglycemia.

Discussion

We have shown before that LCN2 is secreted by osteoblasts to suppress food intake and improve glucose metabolism in lean and obese mice (Mosialou et al., 2017). Herein, we have identified an additional role for LCN2 in obesity: circulating LCN2 levels increase as a protective mechanism to maintain β -cell function and counteract metabolic dysregulation and the adverse effects of obesity and insulin resistance, at least at the early stages of the disease (i.e., prediabetes).

This type of compensatory homeostatic response most probably accounts for the elevated circulating LCN2 levels that have been reported in obese and insulin-resistant states in mice and humans (De la Chesnaye et al., 2015; Wang et al., 2007, 2018; Zhang et al., 2008; Yan et al., 2007; Rashad et al., 2017; Garbacz et al., 2017). Indeed, we found elevated circulating LCN2 levels in obese, prediabetic patients that correlate with BMI and insulin resistance but also β -cell function, indices of healthy glucose metabolism. Interestingly, in patients with established T2D, elevated LCN2 levels are negatively associated with glycated hemoglobin, while there is no association with insulin resistance in nondiabetic, healthy men and women in our studies or in previous observations (Liu et al., 2011; Wang et al., 2018; Wallenius et al., 2011). These results strongly suggest that increased LCN2 levels are a consequence of diabetes in response to the development of insulin resistance at the early stage of the disease and contribute to enhance insulin secretion and limit hyperglycemia. In this compensatory homeostatic role, LCN2 counteracts insulin resistance progression, prevents obesity, and

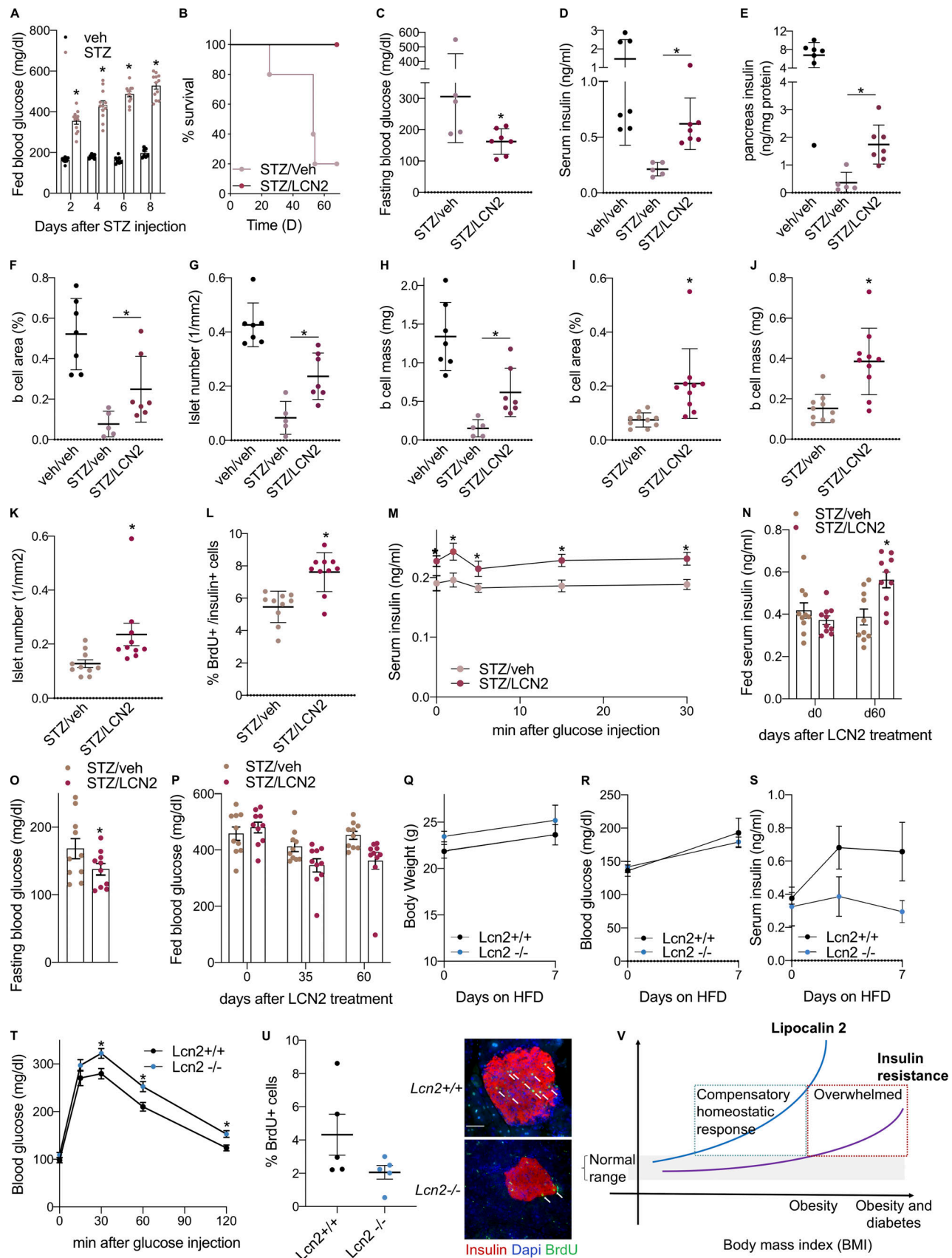


Figure 6. **LCN2 promotes β -cell function in STZ-induced diabetic mice and the early adaptive β -cell proliferation response upon HFD feeding.** (A) Fed blood glucose levels in 9-wk-old WT male mice at the indicated days following vehicle or a single high dose of STZ (150 mg/kg of BW). (B–H) Survival (B),

fasting blood glucose levels (16 d following LCN2 treatment; C), serum insulin levels (D), pancreas insulin content (E), β -cell area (F), islet number (G), and β -cell mass (H) of vehicle ($n = 7$) or STZ-treated mice following treatment with vehicle ($n = 5$) or rLCN2 (150 ng/g/d; $n = 7$) for 2 mo assessed at the time of sacrifice when mice were moribund or at the end of the treatment period for surviving animals. **(I–P)** β -cell area (I), islet number (J), β -cell mass (K), percentage of proliferating β -cells (L), glucose stimulated insulin secretion (M), serum insulin levels (N), fasting (O) and fed (P) blood glucose levels of mice treated with vehicle (Veh) or rLCN2 (150 ng/g/d) for 2 mo following administration of multiple low doses of STZ (50 mg/kg of BW; $n = 10$ /group). **(Q–U)** BW (Q), blood glucose levels (R), serum insulin levels (S), glucose tolerance (T), and percentage of proliferating β -cells (U) in 12-wk-old female *Lcn2*^{-/-} and WT littermates fed an HFD for 1 wk ($n = 5$ /group; arrows indicate BrdU⁺Ins⁺ cells; scale bars, 100 μ m). Data are representative of three independent experiments (A–U). Data are presented as mean \pm SEM. *, $P < 0.05$, Student's *t* test. In B, $P = 0.0039$ (log-rank test). **(V)** Graphical abstract illustrating the endogenous compensatory homeostatic role of LCN2 to face insulin resistance increase, prevent obesity, and avoid diabetes. Once this mechanism is overwhelmed, obesity and diabetes increased sharply. Red box highlights the area where this protective mechanism is overwhelmed by insulin resistance and diabetes starts to rise.

eschews diabetes. Once this mechanism is overwhelmed, obesity increases and diabetes develops (Fig. 6 V).

In accordance with this hypothesis, in all mouse models of obesity and diabetes tested, the increase in circulating LCN2 levels coincides with the onset of insulin resistance. The increase in circulating LCN2 levels is mainly contributed by bone as it was lost in *Lcn2*^{osb}^{-/-} mice placed on HFD. As a result, metabolic dysregulation was more pronounced in HFD-fed *Lcn2*^{osb}^{-/-} mice than in CD-fed *Lcn2*^{osb}^{-/-} mice or HFD-fed WT mice. These observations further substantiate the protective role of LCN2 up-regulation during obesity. Intracellular LCN2 protein levels were decreased in bone and white adipose tissue of obese mice, without measurable changes at the transcriptional level, suggesting enhanced secretion from these tissues as the main mechanism driving the increase in circulating LCN2 levels. An increase in *Lcn2* expression by liver has been reported in obese mice (Zhang et al., 2008), but our data indicate that both *Lcn2* mRNA and protein levels are negligible in liver as compared with bone and therefore unlikely to significantly contribute to elevated circulating LCN2 levels. Although *Lcn2* expression in white adipose tissue is 10-fold lower than in bone, the massive expansion of adipose tissue in *Lepr*^{db/db} and *Lep*^{ob/ob} mice increased the contribution of fat-derived circulating LCN2 levels. It is known that *Lcn2* expression is up-regulated by pro- and anti-inflammatory cytokines (Zhang et al., 2008; Guo et al., 2014; Auguet et al., 2011); therefore, it is possible that the underlying chronic low-grade inflammation in obesity may be the trigger for LCN2 up-regulation.

Cross-sectional studies in humans have suggested an association between LCN2 and obesity or T2D but had not established causality. To address this point, we manipulated LCN2 levels in mice so as to mimic elevated levels during obesity or normalized LCN2 elevated levels during obesity and explored whether these changes could drive diabetes onset or improvement of the metabolic abnormalities, respectively. We found that normalizing serum LCN2 levels in *Lepr*^{db/db} mice or decreasing LCN2 levels in mice fed on HFD worsened their metabolic phenotype by increasing hyperphagia, BW gain, and fat body mass and impairing compensatory islet β -cell hyperplasia. This resulted in decreased insulin secretion and exacerbated hyperglycemia. Accordingly, early β -cell proliferation upon HFD was decreased in the absence of LCN2, resulting in glucose intolerance by day 7. In contrast, elevated LCN2 circulating levels in transgenic mice did not lead to development of obesity and insulin resistance but instead improved their glucose metabolism, fat mass, and food intake and enhanced energy expenditure.

To delineate whether LCN2 independently regulates obesity and β -cell phenotypes, we had previously pair-fed *Lcn2*^{osb}^{-/-} mice to their WT littermates (Mosialou et al., 2017). Pair-feeding normalized BW, fat mass, and insulin sensitivity in *Lcn2*^{osb}^{-/-} mice. However, it did not rescue the impaired glucose-stimulated insulin secretion and serum insulin levels in *Lcn2*^{osb}^{-/-} mice, and as a result, their glucose intolerance persisted. Therefore, we concluded that whereas the anorexigenic function of LCN2 influences fat mass, BW, and insulin sensitivity, its ability to improve glucose tolerance reflects a direct action on pancreatic islets. Mechanistically, we now show that pair-feeding restores the suppression of lipolytic gene expression and the increase in the adipogenic gene expression program in *Lcn2*^{osb}^{-/-} mice. Moreover, treatment of primary pancreatic islets and MIN6 pancreatic β -cells with LCN2 dose-dependently stimulates insulin secretion and β -cell proliferation (Mosialou et al., 2017). Combined, these data suggest that there are two mechanisms involved in the protective role of LCN2 against diabetes, one limiting hyperphagia and thus reducing adiposity and BW and the other directly protecting β -cells and promoting β -cell proliferation. To prove the existence of these two independent mechanisms of action, in this paper, we explored the direct effect of LCN2 on β -cell function using the STZ mouse model of diabetes and the short-term HFD model. The first shows that following β -cell destruction, LCN2 can increase β -cell numbers. The second model shows that within 1 wk of HFD, a time period during which fat mass and BW are not yet increased, LCN2 promotes insulin sensitivity by maintaining β -cell numbers and normal insulin levels.

The proliferative response of β -cells to LCN2 involves regulation of cell cycle components important for β -cell mass expansion. LCN2 acts directly on β -cells to up-regulate the expression of genes promoting cell cycle progression and suppress expression of cell cycle inhibitors. This transcriptional regulation could be secondary to the ability of LCN2 to directly stimulate insulin secretion from β -cells that could in turn enhance glucose and insulin signaling, two key trophic factors during insulin resistance (Jiang et al., 2018; Sachdeva and Stoffers, 2009). Additional effects of LCN2, independent of insulin action, through activation of MC4R signaling (the receptor mediating the appetite suppressing effects of LCN2 in the hypothalamus) or other melanocortin receptors (MC1R, MC3R, and MC5R) that are present in the pancreas (Mansour et al., 2010; Chagnon et al., 1997; Mosialou et al., 2017) and to which we have previously shown that LCN2 can bind (Mosialou et al., 2017) could also be involved and remain to be determined.

Indeed, signaling through melanocortin receptors has been shown to increase cAMP production (Gantz et al., 1993), promote accumulation of intracellular calcium (Newman et al., 2006; Mountjoy et al., 2001), and stimulate PI3K (Ramírez et al., 2015; Vongs et al., 2004) and ERK1/2 activity (Sutton et al., 2005; Daniels et al., 2003). All these pathways are known to promote β -cell proliferation (Linnemann et al., 2014; Jiang et al., 2018).

Besides metabolism, the increase in LCN2 levels with obesity and diabetes could serve as a protective mechanism for bone itself. It is increasingly becoming apparent that excess BW is detrimental to bone mass, strength, and quality, as shown by studies in obese humans and mice on HFD (Goulding et al., 2000; Cao et al., 2009; Hsu et al., 2006). The up-regulation of LCN2 under these states so as to decrease feeding and BW will help prevent undue loading and subsequent fractures of the skeleton. Moreover, the amelioration of diabetes by LCN2 would positively affect the bone fragility reported in T2D patients. Beneficial effects of LCN2 on bone mass have been described before (Capulli et al., 2018; Kim et al., 2015, 2016).

Similar to our studies, others have shown that *Lcn2* expression is up-regulated in the obese state to counteract the impact of increased adiposity/inflammation on fat accumulation and insulin resistance and exert a beneficial role in energy metabolism (Guo et al., 2010, 2012, 2013; Paton et al., 2013; Zhang et al., 2014). In contrast, Law et al. (2010) reported that *Lcn2* knockout mice had decreased obesity. Using the exact same mice, others have shown increased appetite and BW in these mice (Capulli et al., 2018). Similar to these observations and our previous findings, global deletion of *Lcn2* using yet another two mouse models (Paragas et al., 2014; Flo et al., 2004) increased appetite and BW (Fig. S5, A–C). These results provide proof of evidence across all mouse models reported that LCN2 suppresses food intake and BW and improves glucose metabolism.

In summary, we show here a distinct beneficial effect of LCN2 on β -cell function in obese prediabetic and diabetic patients and mouse models of β -cell failure due to toxicity or HFD. At this time, it is not clear whether the initial increase in β -cell hyperplasia to counteract hyperglycemia is protective in the long run, as the model of short-term HFD-induced β -cell hyperplasia is not designed to address the protective contribution of the initial increase in β -cell hyperplasia to the development of insulin resistance. Nevertheless, our experiments show that treatment of obese mice with LCN2 has a maintained, chronic effect in increasing β -cell numbers and improving insulin sensitivity. In addition, the absence of *Lcn2* in *Lcn2^{osb}^{-/-}* mice placed on HFD for long-term (14 wk) deteriorated insulin resistance. The fact that insulin sensitivity is improved in the obesity setting could suggest that LCN2-induced β -cell hyperplasia is beneficial even in states of established insulin resistance. Taken collectively, our observations identify LCN2 as an endogenous compensatory signal to counteract metabolic dysregulation in obesity through its anorexigenic action and by promoting β -cell function.

Materials and methods

Human subjects

Women with prediabetes are part of the Therapeutic Innovation in Type 2 Diabetes (IT-DIAB) prospective cohort conducted by

the Endocrinology Department of the University Research Hospital of Nantes, France (clinicaltrial.gov identifier NCT01218061). This cohort received approval from local Ethic Committee of Nantes, France. Before enrollment, all patients have been clearly and fairly informed and provided written consent. The research has been conducted according to Declaration of Helsinki principles. Inclusion criteria were adults with a prediabetes status corresponding to an impaired fasting blood glucose between 110 mg/dl (6.0 mmol/liter) and 126 mg/dl (7.0 mmol/liter). Exclusion criteria were other endocrine disorders. Patients have been followed annually over 5 yr. Fasting blood glucose and HbA1c were assessed immediately on routine process. Remaining serum and plasma was stored at -80°C . Plasma insulin levels (Cobas automated clinical analyzer system; Roche Diagnostic), plasma high-molecular-weight adiponectin (Fujirebio; electrochemiluminescent enzyme immunoassay on an automated clinical analyzer system, Lumipulse G600) and serum LCN2 (R&D; ELISA kit) were assessed simultaneously for all samples. Homeostatic model assessment is a method to quantify insulin resistance (HOMA-IR) and β -cell function (HOMA-B) using glucose and insulin measurements (molar units). HOMA-IR was calculated as previously described as follows: $\text{glucose} \times \text{insulin} / 22.5$. The formula for HOMA-B (Matthews et al., 1985) is $(20 \times \text{insulin}) / (\text{glucose} - 3.5)$. Primary endpoint was T2D diabetes onset defined as a fasting blood glucose ≥ 1.26 g/liter or a World Health Organization oral GTT ≥ 2 g/liter after 2 h of ingestion.

T2D men and women and non-T2D postmenopausal women were recruited through advertisement flyers. Menopause was defined as no menses for ≥ 3 yr. T2D was defined as HbA1c $\geq 6.5\%$ (according to the International Diabetes Federation Diabetes Atlas 2015; <http://www.diabetesatlas.org>). Duration of diabetes was available for 34 out of 54 T2D postmenopausal women. Subjects were excluded if they had a history of disorders associated with altered skeletal structure or function such as chronic kidney disease, chronic liver disease, active malignancy, acromegaly, Cushing's syndrome, thyroid disease, hyper- or hypoparathyroidism, or organ transplant. Additionally, subjects were excluded if they were currently using teriparatide, estrogen replacement therapy, loop diuretics, anticonvulsive therapies, corticosteroids (>3 wk over the past 3 yr), thiazolidinediones, SGLT2 inhibitors, or anticoagulants. Bisphosphonate and/or denosumab use within the past 12 mo was also an exclusion criterion. Fasting morning blood samples were collected for measurement of LCN2, glucose, insulin, and HbA1c levels. The study was approved by the Columbia University Medical Center Institutional Review Board, and informed written consent was obtained from all participants.

Mice

Lcn2^{-/-} and *Lcn2^{fl/fl}* C57BL/6 mice have been generated by deletion of a 1.9-kb genomic fragment comprising *Lcn2* exons 3–6 as previously described (Mosialou et al., 2017). C57BL/6 *Lcn2^{osb}^{-/-}* mice were generated by crossing *Colla1-Cre* (Dacquin et al., 2002) mice with *Lcn2^{fl/fl}* mice. C57BL/6J (stock number 000664), homozygous and heterozygous leptin receptor-deficient mice (B6.BKS(D)-*Leprdb*/J; stock number 000697), leptin-deficient

mice (B6.Cg-*Lepob*/J; stock number 000632), mice lacking *Mc4r* (B6;129S4-*Mc4r*^{tm1Lowl}/J; stock number 006414), and *Lcn2*^{-/-}(J) mice generated by deletion of exons 2–5 (B6.129P2-*Lcn2*^{tm1Aade}/AkiJ; Flo et al., 2004; stock number 024630) were purchased from The Jackson Laboratory. *Lcn2*^{-/-}(B) mice lacking exons 2–5 were kindly provided by Dr. Jonathan Barasch (Columbia University, New York, NY). Transgenic *Col1a1Lcn2*^{Tg} mice were generated by pronuclei injection of the pJ251.2-*Lcn2* construct harboring full-length *Lcn2* cDNA in fusion with the osteoblast specific fragment of the mouse *type I collagen* promoter into 129/B6 embryos. *Col1a1Lcn2*^{Tg} founder mice were crossed with C57BL/6J WT mice and F1 generation *Col1a1Lcn2*^{Tg} were crossed with C57BL/6J WT mice to obtain *Col1a1Lcn2*^{Tg} and WT littermates (C57BL/6J: 75%; 129/B6:25%) for analyses. *apoELcn2*^{Tg} mice were generated by pronuclei injection of the pLiv.7-*Lcn2* construct harboring full-length *Lcn2* cDNA in fusion with the hepatic control region of the human apolipoprotein E3 gene into 129/B6 embryos. *apoELcn2*^{Tg} founder mice were crossed with C57BL/6J WT mice, and F1 generation *apoELcn2*^{Tg} mice were crossed with C57BL/6J WT mice to obtain *apoELcn2*^{Tg} and WT littermates (C57BL/6J, 75%; 129/B6, 25%) for analyses. HFD-fed mice were given a 60% fat diet (Research Diets; D12492) for 16 wk, 14 wk, or 7 d as indicated. For the 7-d HFD, mice received BrdU (0.8 mg/ml; Sigma) in drinking water on days 3–7. After the seventh day, mice were euthanized and pancreata were processed for analyses. For pair-feeding experiments, mice were individually housed starting at 4 wk of age. Pair-feeding started at 5 wk of age and continued for a period of 8 wk. Food intake was measured daily, and *Lcn2*^{osb}^{-/-} mice were provided every day with the average amount of food consumed by the *Lcn2*^{fl/fl} littermates, which were fed ad libitum on the previous day. To induce β -cell death, 9-wk-old male C57BL6 mice were injected i.p. with a single high dose of STZ (150 mg/kg of BW) or multiple low doses of STZ (50 mg/kg of BW) starting at 6 wk of age daily for five consecutive days. The latter mice were purchased from The Jackson Laboratory. Mice were tested for the development of diabetes (defined as blood glucose level >250 mg/dl), and 1 wk later, they were injected daily i.p. with 150 ng/g mouse recombinant LCN2 or vehicle for 60 d. Recombinant LCN2 was bacterially produced using the pGEX-4T-3 vector in which the cDNA encoding mature mouse LCN2 (residues 83–625) was subcloned into the BamHI and NotI sites (Mosialou et al., 2017). GST-LCN2 fusion protein was purified on glutathione-Sepharose 4B beads and cleaved out from the GST moiety using thrombin, which was subsequently depleted using a HiTrap benzamidin column. Protein purity was assessed by SDS-PAGE followed by Coomassie blue staining. siRNA against LCN2 (sense: 5'-GCUACUGGAUCAAACAUAUAdT-3', antisense: 5'-AAUGUUCUGAUCCAGUAGCdAdT-3'; Dharmacon) was delivered to *Lepr*^{db/db} mice as a complex with a polymer-based reagent (JetPei; in vivo, Polyplus Transfection SA 89129–962) every 2 d for 30 d by s.c. injections. All mice were housed under standard laboratory conditions (12 h on/off; lights on at 7:00) and temperature-controlled environment with food and water available ad libitum apart from pair-feeding experiments. In each experiment, the mice used

were of the same genetic background, as they were all littermates. Mouse genotypes were determined by PCR. All animal procedures were approved by the Columbia University Institutional Animal Care and Use Committee.

Metabolic tests

GTT was performed by i.p. administration of 2 g/kg BW glucose (or 1 g/kg BW in *Lepr*^{db/db} mice) after an overnight fast. Blood glucose was monitored using glucose strips and the Accu-Check Aviva Plus glucometer at 0, 15, 30, 60, and 120 min after glucose injection. A glucose-stimulated insulin secretion test was performed by administration of 3 g/kg BW glucose i.p. after an overnight fast. Serum was collected from tails using heparinized microcapillaries, and insulin was measured at 0, 2, 5, 15, and 30 min by the ultrasensitive mouse insulin ELISA kit (Crystal Chem; 90080). An insulin tolerance test was performed by i.p. administration of 0.5 U/kg BW insulin (or 2.5 U/kg BW in *Lepr*^{db/db} mice) in mice that were fasted for 4 h. Blood glucose levels were measured with the glucometer 0, 15, 30, 60, 90, and 120 min after injection, and percentages of initial blood glucose concentrations are presented. Circulating LCN2 levels were measured by the LCN2 ELISA kit from R&D (MLCN20). TSE Labmaster (TSE Systems) was used for indirect calorimetry and food intake measurements. After ≥ 48 h acclimation to the chambers, data collected over a 48-h period were analyzed as per the manufacturer's recommendations. Body composition was determined using Bruker Minispec nuclear magnetic resonance (Bruker Optics).

Western blotting

Tissue extracts from WT mice were analyzed on SDS-polyacrylamide gel, transferred to a nitrocellulose membrane, and probed with LCN2 (R&D; AF1857) and GAPDH (Cell Signaling Technology; 5174) antibodies following standard procedures. For bone tissue analysis, bone marrow cells were removed completely by flushing extensively the femurs with PBS.

RNA isolation

RNA isolation, cDNA preparation, and real-time PCR analyses were performed following standard protocols. For bone tissue analysis, bone marrow cells were removed completely by extensively flushing the femurs with PBS. Trizol reagent was used for RNA extraction, a random hexamer cDNA synthesis kit (Clontech Laboratories) was used for reverse transcription PCR, and SYBR Green Master Mix (Bio-Rad Laboratories) was used for quantitative PCR. *Actb* was used as an internal control. Data are presented as fold change over control after normalization with *Actb* levels. The following primer sequences were used: *Lcn2* forward: 5'-AGCTTTACGATGTACAGCACCAT-3', reverse: 5'-GATACCTGTGCATATTTCCAG-3'; *Actb* forward: 5'-GACCTCTATGCCAACACAGT-3', reverse: 5'-AGTACTTGCGCTCAGGAGGA-3'; *Ucp1* forward: 5'-GGGCCCTTGTAACAACAAA-3', reverse: 5'-GTCGGTCCTTCCTTGGTGTA-3'; *Pgcl* forward: 5'-CACAAAGACGTCCCTGCTCAGA-3', reverse: 5'-CCTTGGGGTCATTTGGTGACTC-3'; *TNFA* forward: 5'-GAACTGGCAGAAGAGGCACT-3', reverse: 5'-AGGGTCTGGGCCATAGAAGT-3'; *IL-1a* forward: 5'-GCAACGGGAAGATTCTGAAG-3', reverse: 5'-TGA

CAAACCTTCTGCTGACG-3'; *IL-1b* forward: 5'-GCCATCCTCTGT GACTCAT-3', reverse: 5'-AGGCCACAGGTATTTGTGCG-3'; *IL6* forward: 5'-CTGCAAGAGACTTCCATCCAG-3', reverse: 5'-AGT GGTATAGACAGGTCTGTTGG-3'; *C/EBPα* forward: 5'-TGTGAG TTAGCCATGTGGTAGG-3', reverse: 5'-GTCATAACTCCAGTCCC TCTGG-3'; *PPARγ* forward: 5'-GAAACTGGCACCCCTTGAAA-3', reverse: 5'-CCCTGGCAAAGCATTGTAT-3'; *Lpl* forward: 5'-G GGCTATGAGATCAACAAGGTC-3', reverse: 5'-CACTGTGCCGTA CAGAGAAATC-3'; *Tgl* forward: 5'-TATCCGGTGGATGAAAGAGC-3', reverse: 5'-CAGTTCCACCTGCTCAGACA-3'; *Cdkn1a* forward: 5'-CTGTTTCTGTAACATCCTGGTCTG-3', reverse: 5'-TCGAGA AGTATTTATTGAGCACCA-3'; *Cdkn1b* forward: 5'-GCCTGTGTA TGAGAAAAATTGG-3', reverse: 5'-CAACCTTTTAAGCACAGCTA C-3'; *Cdkn2a* forward: 5'-AATCCCAAGAGCAGAGCTAATC-3', reverse: 5'-TTAACAATCCAGCCATTTC-3'; *Cnd2* forward: 5'-GGCTAGAGGTCTGTGAGGAACAA-3', reverse: 5'-TCACAGAGTTG TCGGTGTAAATG-3'; and *Cdk4* forward: 5'-TGGATTTCTTCATG CAACTG-3', reverse: 5'-GAAGAACTTCAGGAGCTCGGTA-3'.

Cell culture and treatment

MC3T3-E1 osteoblastic cells (obtained from ATCC CRL-2593) were maintained in minimum essential medium, alpha modification, supplemented with 10% FBS, 10% L-glutamine, 1% non-essential amino acids, 100 U/ml penicillin, and 100 µg/ml streptomycin and cultured at 37°C in a 5% CO₂ atmosphere. Before treatment, cells were cultured for 4 h in Krebs-Ringer Hepes buffer and then treated with insulin (10 nM) and/or glucose (4.5 g/liter) for 15, 30, or 60 min. Supernatants were collected for the measurement of LCN2 levels by ELISA (R&D; MLCN20). Cells were authenticated by checking mineralization and examining the expression of osteocalcin and bone sialoprotein. MIN6 cells (obtained from ATCC; CRL-11506) were maintained in DMEM (25 mM glucose) supplemented with 2 mM glutamine, 15% FBS, 70 µM β-mercaptoethanol, 100 U/ml penicillin, and 100 µg/ml streptomycin and cultured at 37°C in a 5% CO₂ atmosphere. They were authenticated by examining the expression of insulin and glucagon and testing insulin secretion in response to glucose. For LCN2 treatment and gene expression analysis, cells were cultured overnight in DMEM (5 mM glucose) supplemented with 15% FBS. The next day, cells were starved for 4 h in DMEM (5 mM glucose) and 1% FBS before being treated with various concentrations of LCN2 or vehicle for 4 h. Both cell lines were tested and found to be free of mycoplasma.

Histological analysis

Pancreata were fixed in 10% neutral formalin, embedded in paraffin, and sectioned at 5 µm. Immunohistochemistry was performed using goat anti-insulin (Santa Cruz; SC7839), mouse anti-BrdU (Sigma; B2531), Cy3 rabbit anti-goat IgG (Jackson ImmunoResearch Laboratories; 305-165-045), and Alexa Fluor 488 donkey anti-mouse IgG (Jackson ImmunoResearch Laboratories; 715-545-150) antibodies. Zeiss fluorescence microscope was used, and Ins⁺BrdU⁺ cells were counted manually using ImageJ software. For histomorphometric analysis, Osteomeasure software and a Leica DM 5000B microscope outfitted with a charge-coupled device camera (Sony) were used. Sections were stained with mouse anti-insulin (Santa Cruz; SC8033) and

Vectastain Elite ABC HRP kit (Vector Laboratories; peroxidase, mouse IgG, PK6102).

Statistics

All experiments were repeated at least three times unless stated in the figure legends. Statistical analyses were performed using Prism8 software. Data are presented as mean ± SEM. An unpaired or paired two-tailed Student's *t* test was performed for comparison between two groups and one- or two-way ANOVA for more than two groups comparisons as stated in the figure legends. Normal distribution of the data was examined using the Shapiro-Wilk test for normality. When appropriate, skewed distributed data were log-transformed to meet essential assumptions of inferential statistics. Pearson correlation coefficient was used to assess the association between LCN2 and other studied parameters in prediabetic women after log transformation of the variables. Stepwise linear regression analysis was performed to assess multivariate correlations in diabetic women using the default direction argument. First, dependent variable LCN2 was log-transformed to satisfy distributional assumptions of linear regression. Age, BMI, glucose, insulin, HbA1c, HOMA-β, HOMA-IR, HOMA-S, and dichotomous variable diabetes coded as 0 for individuals with no diabetes and 1 for those with diabetes entered into the stepwise regression analysis. In the final model, derived from stepwise regression and based on the Akaike information criterion, age, BMI, diabetes, HbA1c, insulin, and HOMA-IR were selected as independent determinants of serum LCN2. After fitting the regression model, statistical tests were implemented for ensuring the validity of the estimates of the coefficients obtained. Using the "gvlma" package in R, we performed linear regression diagnostics for validating that our model met the assumptions of normality, independence of errors, linearity, and homoskedasticity. All statistical hypotheses were acceptable. A separate Breusch-Pagan test was also performed, providing strong evidence against heteroscedasticity (Breusch-Pagan = 9.076, *P* value = 0.169). To ensure that the assumption of no or little multicollinearity was met, variance inflation factor scores were computed for each predictor, finding no evidence of collinearity. Lastly, through graphical inspection analysis, residual errors were found to be normally distributed. *P* values < 0.05 were considered to be statistically significant.

Online supplemental material

Fig. S1 shows the positive correlation of LCN2 serum levels with HOMA-B in men with T2D. Fig. S2 shows that increased circulating LCN2 levels in mice overexpressing *Lcn2* in the liver decreases food intake and fat mass and improves glucose metabolism. Fig. S3 shows the normalization of adipogenic and lipolytic gene expression with pair-feeding in *Lcn2^{osb}^{-/-}* mice to their WT littermates and the regulation of cell cycle regulators by LCN2 in pancreatic MIN6 cells. Fig. S4 shows LCN2 circulating levels in STZ diabetic mice and representative images from pancreas sections from HFD-fed *Lcn2^{-/-}* and WT littermates indicating decreased proliferation of β-cells in the absence of LCN2. Fig. S5 shows increased food intake and BW with *Lcn2* deficiency in two different *Lcn2^{-/-}* mouse models. Table S1 shows baseline characteristics of T2D men.

Acknowledgments

We thank Dr. Lori M. Zeltser (Columbia University, New York, NY) for helpful discussions; Dr. Jonathan Barasch (Columbia University) for providing the *Lcn2^{-/-}(B)* mice; and Marina Blanchard, Violette Diery, Marielle Joliveau, Béatrice Lamour, Vincent Jacquin, Matthieu Pichelin, Yassine Zair (CIC Endocrino-Nutrition 1413 INSERM, Centre Hospitalier Universitaire [CHU] Nantes, Nantes, France), Edith Bigot-Corbel (Department of Biochemistry, CHU Nantes), and Marie-Christine Carlier (Département de Biochimie, Hospices Civils de Lyon, France) for their help in data collection of the IT-DIAB study and biological parameter measurements. We also thank the Histology and Metabolic Unit facility of the Diabetes and Endocrinology Research Center (National Institute of Diabetes and Digestive and Kidney Diseases DK063608-07) and the biological resource center for biobanking (CHU Nantes, Hôtel Dieu, Centre de ressources biologiques, Nantes, France; Bioresource Research Impact Factor BB-0033-00040).

This work was supported by the National Institutes of Health (grant P01AG032959 to S. Kousteni and T32 training grant DK07328 to S. Shikhel). IT-DIAB was funded by an OSEO-API (France) ISI grant to Genfit (coordinator of the IT-DIAB consortium) and CHU Nantes, France.

Author contributions: I. Mosialou and S. Kousteni initiated the study, designed experiments, and analyzed data. I. Mosialou, S. Shikhel, N. Luo, P.I. Petropoulou, B. Bisikirska, and R. Tenta performed experiments and analyzed data. N. Luo and N.J. Rothman helped with pancreas histological analysis. K. Panitsas performed statistical analysis of the clinical samples from diabetic patients. B. Cariou, M. Wargny, E. Sornay-Rendu, and C.B. Confavreux collected serum samples, measured biological parameters, and analyzed the data from women with prediabetes in the prospective IT-DIAB cohort study. T.N. and M.R. provided serum samples from patients with T2D. I. Mosialou and S. Kousteni wrote the manuscript. S. Kousteni and C.B. Confavreux directed the research.

Disclosures: B. Cariou reported grants from Amgen, personal fees from AstraZeneca, personal fees from Gilead, personal fees from Novo Nordisk, grants from Regeneron, grants from Sanofi, and personal fees from Sanofi outside the submitted work. No other disclosures were reported.

Submitted: 9 July 2019

Revised: 28 March 2020

Accepted: 15 May 2020

References

- Auguet, T., Y. Quintero, X. Terra, S. Martínez, A. Lucas, S. Pellitero, C. Aguilar, M. Hernández, D. del Castillo, and C. Richart. 2011. Upregulation of lipocalin 2 in adipose tissues of severely obese women: positive relationship with proinflammatory cytokines. *Obesity (Silver Spring)*. 19: 2295–2300. <https://doi.org/10.1038/oby.2011.61>
- Cao, J.J., B.R. Gregoire, and H. Gao. 2009. High-fat diet decreases cancellous bone mass but has no effect on cortical bone mass in the tibia in mice. *Bone*. 44:1097–1104. <https://doi.org/10.1016/j.bone.2009.02.017>
- Capulli, M., M. Ponzetti, A. Maurizi, S. Gemini-Piperni, T. Berger, T.W. Mak, A. Teti, and N. Rucci. 2018. A Complex Role for Lipocalin 2 in Bone Metabolism: Global Ablation in Mice Induces Osteopenia Caused by an Altered Energy Metabolism. *J. Bone Miner. Res.* 33:1141–1153. <https://doi.org/10.1002/jbmr.3406>
- Chagnon, Y.C., W.J. Chen, L. Pérusse, M. Chagnon, A. Nadeau, W.O. Wilkison, and C. Bouchard. 1997. Linkage and association studies between the melanocortin receptors 4 and 5 genes and obesity-related phenotypes in the Québec Family Study. *Mol. Med.* 3:663–673. <https://doi.org/10.1007/BF03401705>
- Dacquin, R., M. Starbuck, T. Schinke, and G. Karsenty. 2002. Mouse α -phal(1)-collagen promoter is the best known promoter to drive efficient Cre recombinase expression in osteoblast. *Dev. Dyn.* 224:245–251. <https://doi.org/10.1002/dvdy.10100>
- Daniels, D., C.S. Patten, J.D. Roth, D.K. Yee, and S.J. Fluharty. 2003. Melanocortin receptor signaling through mitogen-activated protein kinase in vitro and in rat hypothalamus. *Brain Res.* 986:1–11. [https://doi.org/10.1016/S0006-8993\(03\)03162-7](https://doi.org/10.1016/S0006-8993(03)03162-7)
- De la Chesnaye, E., L. Manuel-Apolinar, A. Zarate, L. Damasio, N. Espino, M.C. Revilla-Monsalve, and S. Islas-Andrade. 2015. Lipocalin-2 plasma levels are reduced in patients with long-term type 2 diabetes mellitus. *Int. J. Clin. Exp. Med.* 8:2853–2859.
- Ferron, M., J. Wei, T. Yoshizawa, A. Del Fattore, R.A. DePinho, A. Teti, P. Ducy, and G. Karsenty. 2010. Insulin signaling in osteoblasts integrates bone remodeling and energy metabolism. *Cell*. 142:296–308. <https://doi.org/10.1016/j.cell.2010.06.003>
- Flo, T.H., K.D. Smith, S. Sato, D.J. Rodriguez, M.A. Holmes, R.K. Strong, S. Akira, and A. Aderem. 2004. Lipocalin 2 mediates an innate immune response to bacterial infection by sequestering iron. *Nature*. 432: 917–921. <https://doi.org/10.1038/nature03104>
- Gantz, I., H. Miwa, Y. Konda, Y. Shimoto, T. Tashiro, S.J. Watson, J. DelValle, and T. Yamada. 1993. Molecular cloning, expression, and gene localization of a fourth melanocortin receptor. *J. Biol. Chem.* 268:15174–15179.
- Garbacz, W.G., M. Jiang, M. Xu, J. Yamauchi, H.H. Dong, and W. Xie. 2017. Sex- and Tissue-Specific Role of Estrogen Sulfotransferase in Energy Homeostasis and Insulin Sensitivity. *Endocrinology*. 158:4093–4104. <https://doi.org/10.1210/en.2017-00571>
- Goulding, A., R.W. Taylor, I.E. Jones, K.A. McAuley, P.J. Manning, and S.M. Williams. 2000. Overweight and obese children have low bone mass and area for their weight. *Int. J. Obes. Relat. Metab. Disord.* 24:627–632. <https://doi.org/10.1038/sj.jco.0801207>
- Greig, N.H., H.W. Holloway, K.A. De Ore, D. Jani, Y. Wang, J. Zhou, M.J. Garant, and J.M. Egan. 1999. Once daily injection of exendin-4 to diabetic mice achieves long-term beneficial effects on blood glucose concentrations. *Diabetologia*. 42:45–50. <https://doi.org/10.1007/s001250051111>
- Guo, H., D. Jin, Y. Zhang, W. Wright, M. Bazuine, D.A. Brockman, D.A. Bernlohr, and X. Chen. 2010. Lipocalin-2 deficiency impairs thermogenesis and potentiates diet-induced insulin resistance in mice. *Diabetes*. 59:1376–1385. <https://doi.org/10.2337/db09-1735>
- Guo, H., Y. Zhang, D.A. Brockman, W. Hahn, D.A. Bernlohr, and X. Chen. 2012. Lipocalin 2 deficiency alters estradiol production and estrogen receptor signaling in female mice. *Endocrinology*. 153:1183–1193. <https://doi.org/10.1210/en.2011-1642>
- Guo, H., M. Bazuine, D. Jin, M.M. Huang, S.W. Cushman, and X. Chen. 2013. Evidence for the regulatory role of lipocalin 2 in high-fat diet-induced adipose tissue remodeling in male mice. *Endocrinology*. 154:3525–3538. <https://doi.org/10.1210/en.2013-1289>
- Guo, H., D. Jin, and X. Chen. 2014. Lipocalin 2 is a regulator of macrophage polarization and NF- κ B/STAT3 pathway activation. *Mol. Endocrinol.* 28: 1616–1628. <https://doi.org/10.1210/me.2014-1092>
- Harmon, J.S., M. Bogdani, S.D. Parazzoli, S.S. Mak, E.A. Oseid, M. Berghmans, R.C. Leboeuf, and R.P. Robertson. 2009. beta-Cell-specific overexpression of glutathione peroxidase preserves intranuclear MafA and reverses diabetes in db/db mice. *Endocrinology*. 150:4855–4862. <https://doi.org/10.1210/en.2009-0708>
- Hsu, Y.H., S.A. Venners, H.A. Terwedow, Y. Feng, T. Niu, Z. Li, N. Laird, J.D. Brain, S.R. Cummings, M.L. Bouxsein, et al. 2006. Relation of body composition, fat mass, and serum lipids to osteoporotic fractures and bone mineral density in Chinese men and women. *Am. J. Clin. Nutr.* 83: 146–154. <https://doi.org/10.1093/ajcn/83.1.146>
- Ikeda, N., T. Inoguchi, N. Sonoda, M. Fujii, R. Takei, E. Hirata, H. Yokomizo, J. Zheng, Y. Maeda, K. Kobayashi, et al. 2011. Bileverdin protects against the deterioration of glucose tolerance in db/db mice. *Diabetologia*. 54: 2183–2191. <https://doi.org/10.1007/s00125-011-2197-2>
- Jiang, W.J., Y.C. Peng, and K.M. Yang. 2018. Cellular signaling pathways regulating β -cell proliferation as a promising therapeutic target in the treatment of diabetes. *Exp. Ther. Med.* 16:3275–3285.
- Kanaka-Gantenbein, C., A. Margeli, P. Pervanidou, S. Sakka, G. Mastorakos, G.P. Chrousos, and I. Papassotiropoulos. 2008. Retinol-binding protein 4 and

- lipocalin-2 in childhood and adolescent obesity: when children are not just “small adults”. *Clin. Chem.* 54:1176–1182. <https://doi.org/10.1373/clinchem.2007.099002>
- Kim, H.J., H.J. Yoon, K.A. Yoon, M.R. Gwon, S. Jin Seong, K. Suk, S.Y. Kim, and Y.R. Yoon. 2015. Lipocalin-2 inhibits osteoclast formation by suppressing the proliferation and differentiation of osteoclast lineage cells. *Exp. Cell Res.* 334:301–309. <https://doi.org/10.1016/j.yexcr.2015.03.008>
- Kim, H.J., B. Ohk, W.Y. Kang, S.J. Seong, K. Suk, M.S. Lim, S.Y. Kim, and Y.R. Yoon. 2016. Deficiency of Lipocalin-2 Promotes Proliferation and Differentiation of Osteoclast Precursors via Regulation of c-Fms Expression and Nuclear Factor- κ B Activation. *J. Bone Metab.* 23:8–15. <https://doi.org/10.11005/jbm.2016.23.1.8>
- Law, I.K., A. Xu, K.S. Lam, T. Berger, T.W. Mak, P.M. Vanhoutte, J.T. Liu, G. Sweeney, M. Zhou, B. Yang, et al. 2010. Lipocalin-2 deficiency attenuates insulin resistance associated with aging and obesity. *Diabetes.* 59:872–882. <https://doi.org/10.2337/db09-1541>
- Lee, N.K., H. Sowa, E. Hinoi, M. Ferron, J.D. Ahn, C. Confavreux, R. Dacquin, P.J. Mee, M.D. McKee, D.Y. Jung, et al. 2007. Endocrine regulation of energy metabolism by the skeleton. *Cell.* 130:456–469. <https://doi.org/10.1016/j.cell.2007.05.047>
- Linnemann, A.K., M. Baan, and D.B. Davis. 2014. Pancreatic β -cell proliferation in obesity. *Adv. Nutr.* 5:278–288. <https://doi.org/10.3945/an.113.005488>
- Liu, X., O.P. Hammvik, M. Petrou, H. Gong, J.P. Chamberland, C.A. Christophi, S.N. Kales, D.C. Christiani, and C.S. Mantzoros. 2011. Circulating lipocalin 2 is associated with body fat distribution at baseline but is not an independent predictor of insulin resistance: the prospective Cyprus Metabolism Study. *Eur. J. Endocrinol.* 165:805–812. <https://doi.org/10.1530/EJE-11-0660>
- Liu, D.M., I. Mosialou, and J.M. Liu. 2018. Bone: Another potential target to treat, prevent and predict diabetes. *Diabetes Obes. Metab.* 20:1817–1828. <https://doi.org/10.1111/dom.13330>
- Mansour, M., D. White, C. Wernette, J. Dennis, Y.X. Tao, R. Collins, L. Parker, and E. Morrison. 2010. Pancreatic neuronal melanocortin-4 receptor modulates serum insulin levels independent of leptin receptor. *Endocrine.* 37:220–230. <https://doi.org/10.1007/s12020-009-9289-5>
- Matthews, D.R., J.P. Hosker, A.S. Rudenski, B.A. Naylor, D.F. Treacher, and R.C. Turner. 1985. Homeostasis model assessment: insulin resistance and β -cell function from fasting plasma glucose and insulin concentrations in man. *Diabetologia.* 28:412–419. <https://doi.org/10.1007/BF00280883>
- Mera, P., K. Laue, M. Ferron, C. Confavreux, J. Wei, M. Galán-Díez, A. Lacampagne, S.J. Mitchell, J.A. Mattison, Y. Chen, et al. 2016. Osteocalcin Signaling in Myofibers Is Necessary and Sufficient for Optimum Adaptation to Exercise. *Cell Metab.* 23:1078–1092. <https://doi.org/10.1016/j.cmet.2016.05.004>
- Mera, P., M. Ferron, and I. Mosialou. 2018. Regulation of Energy Metabolism by Bone-Derived Hormones. *Cold Spring Harb. Perspect. Med.* 8. a031666. <https://doi.org/10.1101/cshperspect.a031666>
- Mosialou, I., S. Shikhel, J.M. Liu, A. Maurizi, N. Luo, Z. He, Y. Huang, H. Zong, R.A. Friedman, J. Barasch, et al. 2017. MC4R-dependent suppression of appetite by bone-derived lipocalin 2. *Nature.* 543:385–390. <https://doi.org/10.1038/nature21697>
- Mountjoy, K.G., P.L. Kong, J.A. Taylor, D.H. Willard, and W.O. Wilkison. 2001. Melanocortin receptor-mediated mobilization of intracellular free calcium in HEK293 cells. *Physiol. Genomics.* 5:11–19. <https://doi.org/10.1152/physiolgenomics.2001.5.1.11>
- Nakagawa, T., A. Tsuchida, Y. Itakura, T. Nonomura, M. Ono, F. Hirota, T. Inoue, C. Nakayama, M. Tajji, and H. Noguchi. 2000. Brain-derived neurotrophic factor regulates glucose metabolism by modulating energy balance in diabetic mice. *Diabetes.* 49:436–444. <https://doi.org/10.2337/diabetes.49.3.436>
- Newman, E.A., B.X. Chai, W. Zhang, J.Y. Li, J.B. Ammori, and M.W. Mulholland. 2006. Activation of the melanocortin-4 receptor mobilizes intracellular free calcium in immortalized hypothalamic neurons. *J. Surg. Res.* 132:201–207. <https://doi.org/10.1016/j.jss.2006.02.003>
- Ono, M., J. Ichihara, T. Nonomura, Y. Itakura, M. Tajji, C. Nakayama, and H. Noguchi. 1997. Brain-derived neurotrophic factor reduces blood glucose level in obese diabetic mice but not in normal mice. *Biochem. Biophys. Res. Commun.* 238:633–637. <https://doi.org/10.1006/bbrc.1997.7220>
- Paragas, N., R. Kulkarni, M. Werth, K.M. Schmidt-Ott, C. Forster, R. Deng, Q. Zhang, E. Singer, A.D. Klose, T.H. Shen, et al. 2014. α -Intercalated cells defend the urinary system from bacterial infection. *J. Clin. Invest.* 124:2963–2976. <https://doi.org/10.1172/JCI71630>
- Paton, C.M., M.P. Rogowski, A.L. Kozimor, J.L. Stevenson, H. Chang, and J.A. Cooper. 2013. Lipocalin-2 increases fat oxidation in vitro and is correlated with energy expenditure in normal weight but not obese women. *Obesity (Silver Spring).* 21:E640–E648. <https://doi.org/10.1002/oby.20507>
- Ramírez, D., J. Saba, L. Carniglia, D. Durand, M. Lasaga, and C. Caruso. 2015. Melanocortin 4 receptor activates ERK-cFos pathway to increase brain-derived neurotrophic factor expression in rat astrocytes and hypothalamus. *Mol. Cell. Endocrinol.* 411:28–37. <https://doi.org/10.1016/j.mce.2015.04.008>
- Rashad, N.M., A.S. El-Shal, R.L. Etewa, and F.M. Wadea. 2017. Lipocalin-2 expression and serum levels as early predictors of type 2 diabetes mellitus in obese women. *IUBMB Life.* 69:88–97. <https://doi.org/10.1002/iub.1594>
- Rolin, B., M.O. Larsen, C.F. Gotfredsen, C.F. Deacon, R.D. Carr, M. Willen, and L.B. Knudsen. 2002. The long-acting GLP-1 derivative NN2211 ameliorates glycemia and increases β -cell mass in diabetic mice. *Am. J. Physiol. Endocrinol. Metab.* 283:E745–E752. <https://doi.org/10.1152/ajpendo.00030.2002>
- Sachdeva, M.M., and D.A. Stoffers. 2009. Minireview: Meeting the demand for insulin: molecular mechanisms of adaptive postnatal β -cell mass expansion. *Mol. Endocrinol.* 23:747–758. <https://doi.org/10.1210/me.2008-0400>
- Stamateris, R.E., R.B. Sharma, D.A. Hollern, and L.C. Alonso. 2013. Adaptive β -cell proliferation increases early in high-fat feeding in mice, concurrent with metabolic changes, with induction of islet cyclin D2 expression. *Am. J. Physiol. Endocrinol. Metab.* 305:E149–E159. <https://doi.org/10.1152/ajpendo.00040.2013>
- Sutton, G.M., B. Duos, L.M. Patterson, and H.R. Berthoud. 2005. Melanocortinergic modulation of cholecystokinin-induced suppression of feeding through extracellular signal-regulated kinase signaling in rat solitary nucleus. *Endocrinology.* 146:3739–3747. <https://doi.org/10.1210/en.2005-0562>
- Thorkildsen, C., S. Neve, B.D. Larsen, E. Meier, and J.S. Petersen. 2003. Glucagon-like peptide 1 receptor agonist ZPI0A increases insulin mRNA expression and prevents diabetic progression in db/db mice. *J. Pharmacol. Exp. Ther.* 307:490–496. <https://doi.org/10.1124/jpet.103.051987>
- Trevaskis, J.L., and A.A. Butler. 2005. Double leptin and melanocortin-4 receptor gene mutations have an additive effect on fat mass and are associated with reduced effects of leptin on weight loss and food intake. *Endocrinology.* 146:4257–4265. <https://doi.org/10.1210/en.2005-0492>
- Vongs, A., N.M. Lynn, and C.I. Rosenblum. 2004. Activation of MAP kinase by MC4-R through PI3 kinase. *Regul. Pept.* 120:113–118. <https://doi.org/10.1016/j.regpep.2004.02.018>
- Wallenius, V., E. Elias, G.M. Bergstrom, H. Zetterberg, and C.J. Behre. 2011. The lipocalins retinol-binding protein-4, lipocalin-2 and lipocalin-type prostaglandin D2-synthase correlate with markers of inflammatory activity, alcohol intake and blood lipids, but not with insulin sensitivity in metabolically healthy 58-year-old Swedish men. *Exp. Clin. Endocrinol. Diabetes.* 119:75–80. <https://doi.org/10.1055/s-0030-1265212>
- Wang, Y., K.S. Lam, E.W. Kraegen, G. Sweeney, J. Zhang, A.W. Tso, W.S. Chow, N.M. Wat, J.Y. Xu, R.L. Hoo, et al. 2007. Lipocalin-2 is an inflammatory marker closely associated with obesity, insulin resistance, and hyperglycemia in humans. *Clin. Chem.* 53:34–41. <https://doi.org/10.1373/clinchem.2006.075614>
- Wang, W., S. Ye, L. Qian, Y. Xing, A. Ren, C. Chen, S. Li, J. Xu, Q. Liu, L. Dong, et al. 2018. Elevated serum lipocalin 2 levels are associated with indexes of both glucose and bone metabolism in type 2 diabetes mellitus. *Endocrinology.* 169:276–282. <https://doi.org/10.5603/EP.a2018.0030>
- Wei, J., T. Hanna, N. Suda, G. Karsenty, and P. Ducy. 2014. Osteocalcin promotes β -cell proliferation during development and adulthood through Gprc6a. *Diabetes.* 63:1021–1031. <https://doi.org/10.2337/db13-0887>
- Yan, Q.W., Q. Yang, N. Mody, T.E. Graham, C.H. Hsu, Z. Xu, N.E. Houstis, B.B. Kahn, and E.D. Rosen. 2007. The adipokine lipocalin 2 is regulated by obesity and promotes insulin resistance. *Diabetes.* 56:2533–2540. <https://doi.org/10.2337/db07-0007>
- Yoo, H.J., H.J. Hwang, T.W. Jung, J.Y. Ryu, H.C. Hong, H.Y. Choi, S.H. Baik, and K.M. Choi. 2014. Adipose gene expression profiles related to metabolic syndrome using microarray analyses in two different models. *Diabetes Metab. J.* 38:356–365. <https://doi.org/10.4093/dmj.2014.38.5.356>
- Yoshikawa, Y., A. Kode, L. Xu, I. Mosialou, B.C. Silva, M. Ferron, T.L. Clemens, A.N. Economides, and S. Kousteni. 2011. Genetic evidence points to an osteocalcin-independent influence of osteoblasts on energy metabolism. *J. Bone Miner. Res.* 26:2012–2025. <https://doi.org/10.1002/jbmr.417>
- Zhang, J., Y. Wu, Y. Zhang, D. Leroith, D.A. Bernlohr, and X. Chen. 2008. The role of lipocalin 2 in the regulation of inflammation in adipocytes and macrophages. *Mol. Endocrinol.* 22:1416–1426. <https://doi.org/10.1210/me.2007-0420>
- Zhang, Y., H. Guo, J.A. Deis, M.G. Mashek, M. Zhao, D. Ariyakumar, A.G. Armien, D.A. Bernlohr, D.G. Mashek, and X. Chen. 2014. Lipocalin 2 regulates brown fat activation via a nonadrenergic activation mechanism. *J. Biol. Chem.* 289:22063–22077. <https://doi.org/10.1074/jbc.M114.559104>

Supplemental material

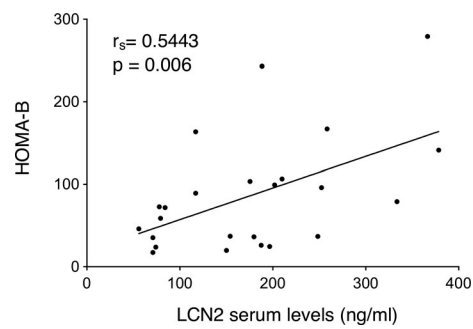


Figure S1. **Circulating LCN2 levels correlate with β -cell function in men with T2D.** Spearman correlation of morning fasting LCN2 serum levels with HOMA-B in men with T2D ($n = 24$).

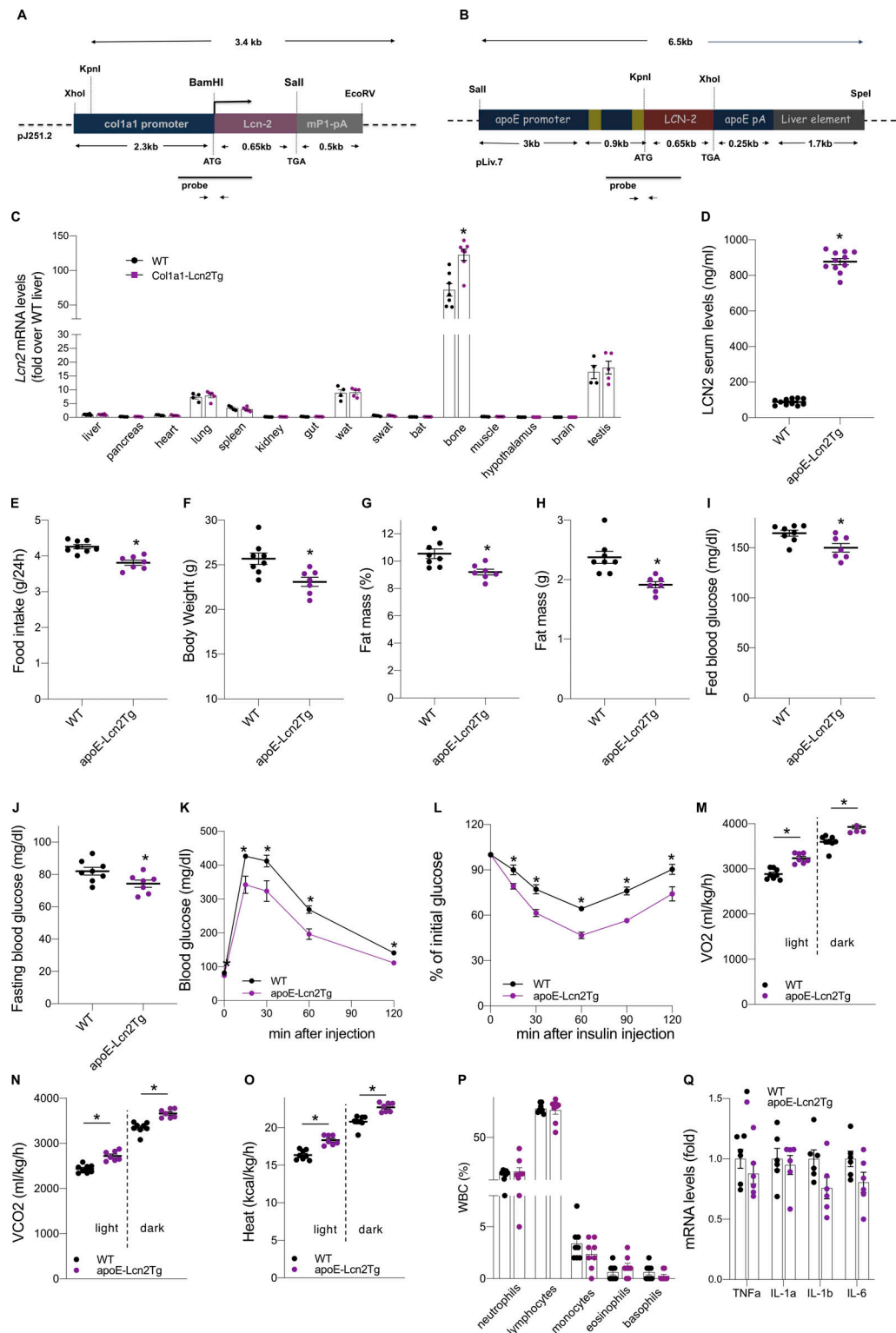


Figure S2. Increased circulating LCN2 levels in mice overexpressing *Lcn2* in the liver decreases food intake and fat mass and improves glucose metabolism. (A and B) Schematic illustration of the *Col1a1-Lcn2* transgenic construct (A) and *apoE-Lcn2* transgenic construct (B) used to generate *Col1a1-Lcn2*^{Tg} and *apoE-Lcn2*^{Tg} transgenic mice, respectively. Location of probes used for Southern blotting and primers used for PCR to detect the transgene are indicated. (C) Tissue expression of *Lcn2* in 10-wk-old *Col1a1-Lcn2*^{Tg} (n = 5) and WT (n = 4) littermate male mice. In bone and liver, n = 7/group. Expression levels are plotted relative to their expression levels in the liver of WT mice. (D) Serum LCN2 levels in 12-wk-old *apoE-Lcn2*^{Tg} and WT littermate male mice (n = 11/group). (E–Q) Food intake (E), BW (F), fat body mass (percentage of total body mass; G), fat body mass (grams; H), fed (I) and fasting (J) blood glucose levels, glucose tolerance (K), insulin sensitivity (L), O₂ consumption, CO₂ production (N), heat production (O), white blood cell counts (n = 8/group; P) and relative expression levels of TNFα, IL1α, IL1β, and IL6 (Q) in white adipose tissue (n = 6/group) of 12-wk-old *apoE-Lcn2*^{Tg} and WT littermate male mice. In E–O, WT, n = 8; *apoE-Lcn2*^{Tg}, n = 7. Data are representative of three independent experiments (A–Q). Data are presented as mean ± SEM. *, P < 0.05, Student's *t* test.

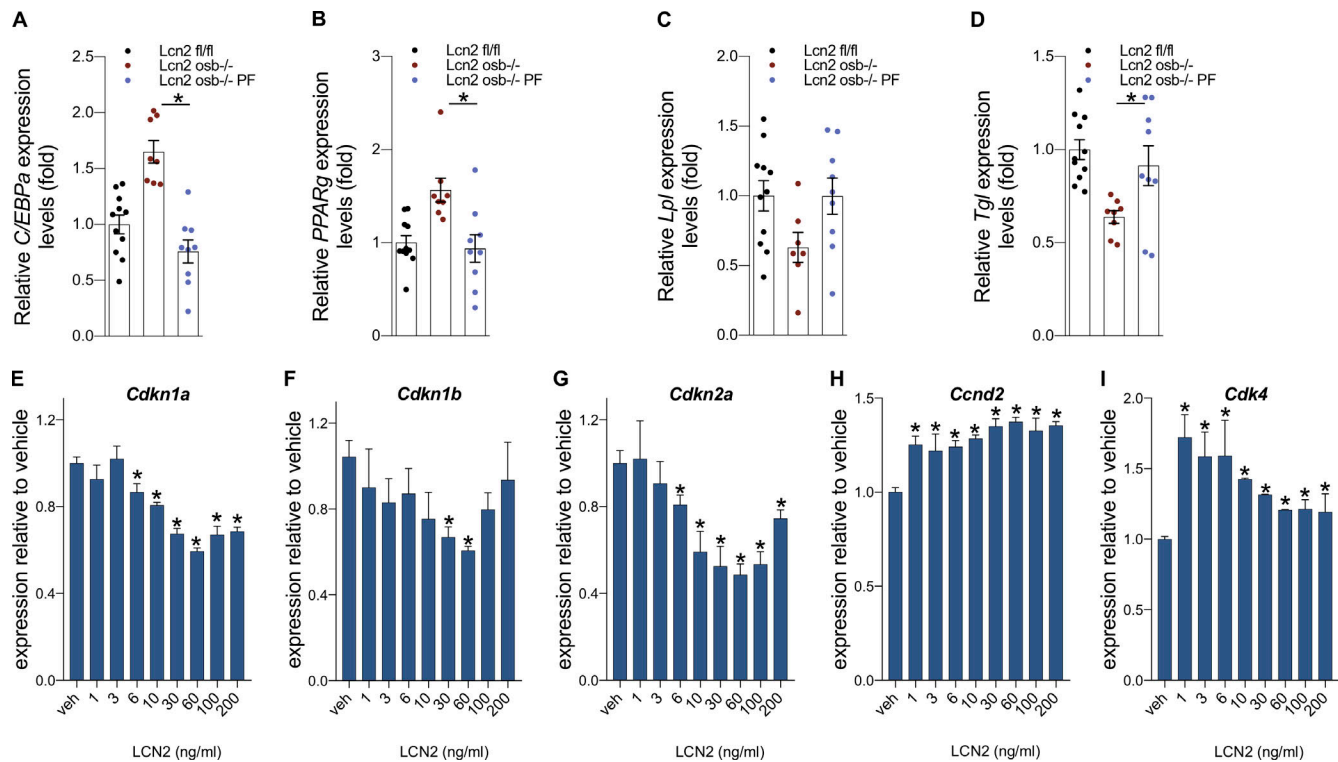


Figure S3. **LCN2 indirectly regulates adiposity while it directly acts on pancreatic β -cells to regulate β -cell proliferation at the transcriptional level.** (A–D) Real-time PCR analysis of adipogenic (A and B) and lipolytic genes (C and D) in pair-fed (PF) male *Lcn2_{osb}^{-/-}* mice ($n = 9$) to their WT littermates ($n = 11$) as compared with ad libitum-fed *Lcn2_{osb}^{-/-}* mice ($n = 8$). *, $P < 0.05$, one-way ANOVA. (E–I) Cell cycle expression genes in pancreatic MIN6 cells treated with increasing doses of LCN2 for 4 h. Data are representative of three independent experiments (A–I). Data are presented as mean \pm SEM. *, $P < 0.05$, Student's t test.

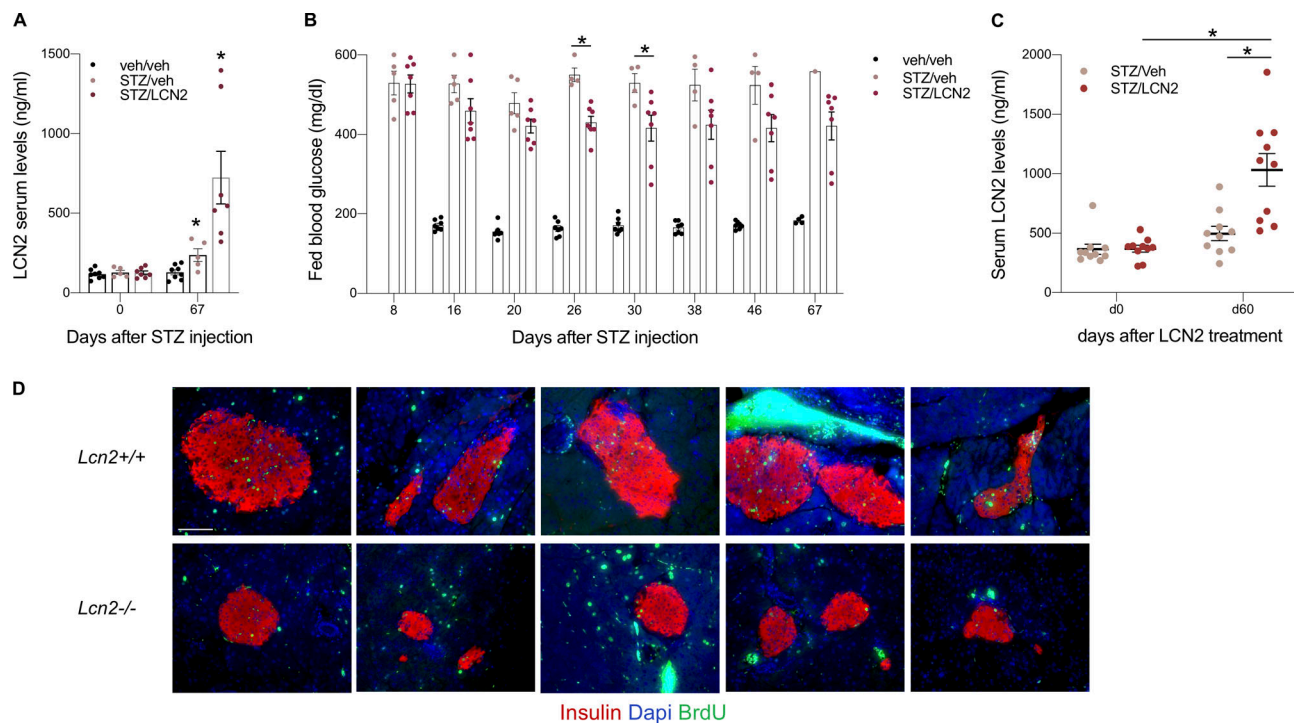


Figure S4. **LCN2 increases with diabetes in STZ-induced diabetic mice and promotes the early adaptive β -cell proliferation response upon HFD feeding.** (A and B) Serum LCN2 levels (A) and fed blood glucose levels (B) of mice treated with rLCN2 ($n = 7$) or vehicle ($n = 5$) for 2 mo following a single high dose of STZ or vehicle ($n = 7$). (C) Serum LCN2 levels in mice treated with rLCN2 or vehicle following multiple low doses of STZ ($n = 10$ /group). (D) Representative images from pancreas sections following insulin and BrdU immunostaining from 12-wk-old female *Lcn2*^{-/-} and WT littermates fed on HFD for 1 wk ($n = 5$ /group; scale bars, 100 μ m). Data are representative of three independent experiments (A–D). Data are presented as mean \pm SEM. *, $P < 0.05$, two-way ANOVA.

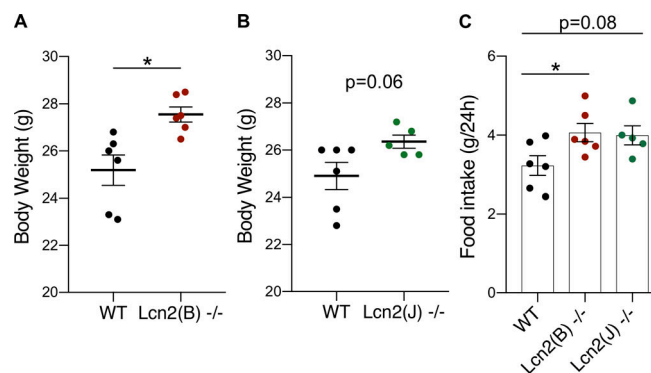


Figure S5. ***Lcn2* deficiency increases food intake and BW in two different *Lcn2*^{-/-} mouse models.** (A–C) BW (A and B) and daily food intake (C) of 12-wk-old male *Lcn2*^{-/-}(B) ($n = 6$; A and C) and *Lcn2*^{-/-}(J) ($n = 5$; B and C) mice and WT littermate controls ($n = 6$). Data are representative of three independent experiments (A–C). Data are presented as mean \pm SEM. *, $P < 0.05$, Student's t test.

Table S1 is provided online as a separate Word document and shows baseline characteristics of T2D men.